

University of Missouri
Columbia, Missouri
College of Agriculture
Agricultural Experiment Station
Roger L. Mitchell, Director

Effective Soil Water Potential for a Steady, Radial-Axial Flow System

W.R. Teague, K.M. Hassan, A.H. Barakah



Acknowledgements

Thanks to each of the following organizations for financial support of research leading to this manuscript.

University of Missouri, Columbia
City of Columbia, Missouri
Missouri Department of Natural Resources
Federal Office of Water Resources Research

Thanks to each of the following for financial assistance in completing the manuscript.

Donald and Barbara Osburn
Walter and Gloria Teague
Bill and Peggy Windsor

I am grateful for help received from several besides those already mentioned. "Thank you" is too little, but it is a beginning.

To Joe Ritchie for introducing me to soil science, and to Kirk Brown for providing much opportunity as I studied transport processes. I am likewise indebted to James Bradford and David Hughes, not only for insights they provided into the world of mathematics, but for inspiration to try.

To Calvin Ahlbrandt, whose patient listening and enthusiasm helped me order my thoughts for writing. Special thanks to Anita Blanchar, whose skill, persistence, and efficiency in typing the manuscript, brought order out of chaos and the work to fruition. Likewise, Paul Koenig's assistance with computing was invaluable, and so was his willing spirit and clear thinking in the face of all kinds of confusion.

To Bob Blanchar, Joe Bradford, and Clarence Scrivner, who showed me what research is about and led me to some meaningful questions in the science of soil-root systems. I owe much to them as good fellow soldiers, but more than that, as my teachers.

As I worked on the manuscript, I received help from several Christians in Columbia, Boonville, and Fayette, Missouri. Especially, Jerry and Claudia Templer and Ben and Marcia Rogers extended friendship and shelter when I despaired of life. The soul and the strength to complete this work came with them, as "on the wings of eagles."

Love, special honor, and thanks for waiting, to my wife Rebecca, and to my daughters, Lisa, Leslie, and Lynn. Every one made me ashamed of myself by carrying more than her fair share of the family load!

To the One whose ways are better than ours: Thank you, Lord, for everything!

W.R.T.

Contents

	Page
Effective Soil Water Potential For A Steady, Radial-Axial Flow System	7
Hydraulic Resistance Equations	8
The Flow System And Boundary Value Problem	13
Green's Function Solution	15
System Flow Equation	20
The Effective Potential And Effective Conductance	20
Back-Transformation Equations	22
The System For Constant \bar{h} And \bar{k}_x	24
Concluding Remarks	31
References	35
Appendix	
A List of Symbols	38
B The Back-Transformation Equations	41
C Program For Constant \bar{h} And \bar{k}_x	41
D Program For Constant \bar{k}_x	42
E Qualitative Analysis	68

Effective Soil Water Potential for a Steady, Radial-Axial Flow System

W. R. Teague, K. M. Hassan, and A. H. Barakah

As water moves from the soil in the rhizosphere, to the plant canopy during transpiration, it incurs a loss in potential energy that may be attributed to flow impedances offered by the soil, and by various tissues throughout the root system. The impedances, like the soil and plant factors on which they depend, are dynamic and spatially variable. At a given time, the magnitude and spatial distribution of the soil-root system flow impedance combine with the magnitude and spatial distribution of the soil-water potential to govern the relationship between the plant's water supply flux and hydraulic potential. What follows in this bulletin is a linear, steady-flow model of water transport that focuses on the spatial arrangement of impedances, as they are encountered by water during its absorption into a root, and during its subsequent conduction within the root vascular system.

Research leading to the model was encouraged by earlier work (Kiniry et al., 1983; Blanchar et al., 1978; Bradford and Blanchar, 1980; Jordan and Ritchie, 1971; Taylor, 1983; Jung and Taylor, 1984) characterizing soil influences on root growth, plant water supplies, and productivity of agronomic systems. The hydraulic potential and flux of water delivered to the canopy by a plant's root system are fundamental water supply variables, and they are jointly controlled by soil, plant, and atmospheric factors. In spite of canopy and atmospheric controls on the flux and potential, it is reasonable to consider a functional relationship among the flux, the potential, and the controlling soil and root system variables, as a basis for studying the plant water supply. Recently, Jung and Taylor (1984) used a multistage, series-parallel hydraulic resistance model to study the influences of soil water content, root spacing, and the numbers and diameters of main root xylem vessels on water relations of field grown soybeans. That model is a lumped parameter counterpart of the distributed parameter model considered here. Both models lead to algebraic system flow equations. Both equations state that the water flux out of the system is proportional to the difference between the hydraulic potential at the system's outflow boundary, and an effective, weighted-average soil water potential. The potential is effective in the sense of an Ohm's Law analogy.

The present model is based on a two-point boundary value problem in a one-dimensional curvilinear space frame. The problem was constructed from a flow hypothesis (Cowan and Milthorpe, 1968) consisting of two coupled, linear first-order differential equations. The manner in which the equations are coupled preserves a radial-axial flow geometry that is common to plant root systems. Similar transport problems are discussed elsewhere (Carslaw and Jaegar, 1959), but the integral solution presented here is the only one we are aware of that accounts for position dependence in the system's lateral boundary potential, and in both transport properties.

The specifications for the radial-axial flow region, the boundary value problem, the Green's function solution, the derivation of the algebraic system transport equation, closed-form and numerical solutions of the problem for special cases, and computer programs of the solutions are included in this bulletin.

Of particular significance from the present point of view is the algebraic Ohm's Law representation of the flux out of the system. In this equation, the difference between a weighted integral of the position-dependent soil water potential and the axial hydraulic potential at the outflow boundary drives the flux. The weighting function that generates this effective soil water potential depends in a uniquely prescribed manner on the system's two position-dependent transport properties. The effective conductance, which is the proportionality constant for the system flow equation, also depends in a uniquely prescribed manner on the two transport properties. For this reason the equation is referred to as pathway specific to distinguish it from an important class of equations in which the variables do not depend explicitly on soil or root system sources of impedance.

The model was derived in a dimensionless space frame after a linear transformation of variables. It is presented here without direct reference to the specific nature of the soil physical or root physiological sources of impedance. It was used to study the impact of the magnitude and spatial distribution of the system's radial transfer coefficient (transport property controlling absorption) on the axial flux and potential distributions, the effective system conductance, and the effective soil water potential for a constant axial conductivity and linear soil water potential distribution. The results of that study are presented graphically.

Hydraulic Resistance Equations

Equations having the general form:

$$q = (\psi_1 - \psi_2)/R \quad [1]$$

have provided the starting point for many investigations of soil-plant water flow phenomena. They incorporate the assumption that the water flux, q , through some specified region of a soil-plant system is proportional to the difference between the water potential, ψ_1 , at one extremity of the flow region being analyzed, and ψ_2 , the potential at the opposing extremity. In applications of this equation to intact systems, ψ_1 has corresponded to the soil water potential in the plant root zone, and ψ_2 to the plant's leaf water potential. Usually q in such instances, was identified with the average transpiration flux over a specified time period, and R the combined soil-plant hydraulic resistance.

Interest in this equation stems from agronomic, as well as hydrologic concerns. Aside from its claim of an elegantly simple representation of an exceedingly complex flow system, the variables ψ_2 and q can provide important clues to a plant's internal water status in relation to growth and

productivity. The water potential carries information about hydraulic pressures which aid in the mechanical support of leaves and stems, and which also aid in cell expansions that accompany the growth of various plant components. It is also related to physiological stomatal controls by which influxes of carbon dioxide, from the atmosphere, and transpiration, are simultaneously regulated (Hsiao and Acevedo, 1974). In situations where plant water deficits have been primarily responsible for observed yield variations, certain functions of the transpiration flux, q , have been correlated with various measures of productivity in field studies (Hanks, 1983; Sudar et al., 1981). The equation is therefore a potentially powerful modeling tool, not only for purely descriptive purposes, but also as an aid for better understanding and improving agronomic systems (Feddes, 1981). For example, if ψ_1 and R can be quantitatively related to soil and root system properties which affect ψ_2 and q , then models based on [1] are likely to prove useful for assessing and predicting productivity gains like the ones observed by Bradford and Blanchar (1980). Their soil profile modification schemes led to remarkable sorghum yield increases on the fragipan soil they studied. They linked observed yield increases over a three year period directly to enhanced root growth (Blanchar et al., 1978), and augmented water supplies (Bradford and Blanchar, 1980), both of which occurred as a result of their physical and chemical alterations of the soil.

In spite of its simplicity and intuitive appeal, modeling soil-plant water transport with Equation [1] is not straightforward. At best, it provides an approximately quantitatively correct representation of the water phenomena that have been observed in field and laboratory studies. Its mathematical structure carries certain implications that are not strictly true over ranges of conditions commonly encountered (Cowan, 1965; Gardner, 1968). Consequently, the equation has carried a stigma of difficult-to-quantify uncertainty, while it has provided much of the basis for modeling soil-plant water phenomena for many years. Particular implications of the mathematical structure that are not rigorously met in field and laboratory systems follow.

- (1) It implies steady flow. The variables R , ψ_1 , ψ_2 and q are independent of time. In field and laboratory systems, diurnal and longer term variations in potentials and fluxes are common (Kozlowski, 1968; Ehlers et al., 1981). The diurnal fluctuations accompany the periodicity of atmospheric factors that are either related to the energy supply for evaporation, or else related to the transport of water away from the canopy (Slatyer, 1967; van Bavel, 1967). Diurnal, or even shorter term, variations in stomatal aperture are common as well, and function interactively with the plant water supply (Cowan and Milthorpe, 1968), in contributing to the time dependence of observed transpiration rates and water potentials. Changes in the diurnal patterns also accompany the dynamics of

soil, root system, canopy, and atmospheric factors over periods of days to weeks or longer.

- (2) In Equation [1], the potentials ψ_1 and ψ_2 appear as single values, with ψ_1 representing the soil and ψ_2 the plant. The conjecture that ψ_1 and ψ_2 are both independent of position leads to the conclusion that R arises solely from impedances to water transfer at the soil-root interface. This region may in fact present considerable impedance to absorption (Herkelrath et al., 1977). However, potential differences internal to both the plant and the soil accompany water flow from soil to atmosphere, and spatial variability in both variables is frequently observed.
- (3) Equation [1] is linear. Soil water flow is recognized as a generally non-linear process which defies linear analysis unless a relatively narrow range of water potentials accompanies the movement. It is conceivable that the non-linearity associated with water uptake from the soil would also affect relationships that are detected among the variables ψ_1 , ψ_2 and q . Moreover, there is good reason to believe that flow cross sections in plant xylem vessels are diminished at lower water potentials, as a result of cavitation in the water columns that can occur in those vessels at high tension (Milburn, 1979). If this is the case the plant may also be a source of non-linearity of the flow.
- (4) Equation [1] implies a homogeneity of the potentials which operate in the system, in the sense that any component potentials of ψ_1 and ψ_2 influence the flux through the same resistance, R . This supposition appears unlikely to hold in systems where the osmotic potential and the hydraulic potential are simultaneously active in the water transport process (Cowan and Milthorpe, 1968; Corey and Klute, 1985). Both these potentials are operative to one degree or another in virtually all soil-plant systems.

It is principally the interpretation of slowly varying and spatially non-uniform soil water potentials, and their representation as a single-valued effective potential, in the sense of ψ_1 in Equation [1], with which this paper is concerned. The analysis which follows later will be confined to steady-flow conditions, with a uniformly zero osmotic potential.

Before proceeding with the main point, the following remarks are directed philosophically toward empirical uses of the hydraulic resistance equation, in the light of the above mentioned uncertainties regarding its qualifications.

Earlier investigations that were organized around the soil-plant resistance concept have provided a great deal of insight into the water-related behavior of these systems. This is in spite of the discrepancy between assumptions about the flow, that are required to rigorously support the use of the equation, and the often encountered conditions. It is not within our grasp at the present to either analyze or effectively argue those circum-

stances under which it is most likely to be useful, as opposed to those under which the equation might be treacherously misleading. We are convinced that both these categories of circumstances exist, and various strategies have been devised for empirically adapting the equation. We salute those people who have studied the system and made the measurements, and hope the work described here will be helpful in some future experimental investigations.

Equation [1] will be most useful when its strengths, and its limitations, are recognized and respected. Its linearity, which has been cited as a weakness, also lends it a great deal of power in tracking complex flow geometries, when the experimental conditions and underlying assumptions of the equation are compatible.

In recent years, several investigators have used the hydraulic resistance equation as a basis for exploring soil and root system influences on the plant water supply (Gardner, 1968; Cowan and Milthorpe, 1968; Klepper and Taylor, 1978; Jung and Taylor, 1984). In that context the focus is on the soil-root subsystem, rather than on the whole soil-plant system. The water potential ψ_2 corresponds to the xylem water potential at the junction between the root system and the plant stem. The water potential in that region has been referred to as the plant's crown potential ψ_c (Klepper and Taylor, 1978). Experimentally, values of water potential determined on covered leaves near the stem base are thought to provide acceptable approximations to ψ_c on some plants. Klepper (1983) pointed out that in many plants, anastomosis of xylem vessels at the stem base provides for free exchange of water and therefore a uniform crown potential is a reasonable assumption. She further observed that is not always the case, because certain trees, for example, exhibit non-uniform xylem potentials at the bases of their trunks (Klepper, 1983; Ginter-Whitehouse et al., 1983).

Water transport that occurs in soil-root subsystems passes through two distinct stages in its progress from the soil toward the root crown. The flows associated with the two stages are widely disparate in several respects (Cowan and Milthorpe, 1968; Klepper, 1983). In the absorption stage (radial pathway) water migrates relatively short distances through the soil and then passes through various root tissues before entering a xylem vessel. In the axial stage (axial pathway) it moves, on the average, much longer distances through xylem vessels to the root crown. A qualitative comparison between various characteristics of the flow in the two stages is made in Table 1. Potential gradients that occur in the axial stage are thought to be small in comparison to those which occur in the absorption stage (Klepper, 1983). However, the contribution of axial potential differences to the overall difference in potential between the soil in a given region, and the root crown is uncertain. Klepper and Taylor (1978) and Klepper (1983) presented compelling arguments for possibly significant variations in the xylem potential.

Table 1.
Qualitative comparison of flow variables in a
soil-root system water movement pathway.

PATHWAY	Radial		Axial
LENGTH	$\Delta\sigma_r$	\ll	$\Delta\sigma_x$
CROSS SECTION	A_r	\gg	A_x
POTENTIAL GRADIENT	$ \partial\psi/\partial\psi _r$	\gg	$ \partial\psi/\partial\psi _x$
TOTAL POTENTIAL DROP [†]	$\Delta\psi_r$	$>$	$\Delta\psi_x$
FLUX DENSITY	f_r	\ll	f_x

[†]Appears to be consensus among researchers at the present time.

Recently Jung and Taylor (1984) presented a lumped hydraulic resistance model of a soil-root system water flow which explicitly recognizes both the soil and root impedances to radial flow in the absorption stage, and also recognizes impedances encountered in the axial stage. They presented a formula for the system's effective soil water potential, which is a weighted average of the spatially varying soil water potential in the root zone. The mathematical expression of the flow, in the multistage series-parallel resistance model, consists of a set of linear algebraic equations in the water flux, the xylem potential, and the soil water potential. The entire system of equations can be represented by Equation [1] with the effective soil water potential in the place of ψ_1 and the crown potential in the place of ψ_2 . The formula for the effective soil water potential was derived from the set of algebraic equations. Their work stimulated our further consideration of related discussions of the underlying theory. In particular, we found that Cowan and Milthorpe (1968) described the axial and absorption stages of flow on two different scales. They pointed out the lateral augmentation of the axial flux which occurs as water is absorbed by a single root, and a similar radial-axial flow configuration which accompanies water transport in an entire root system. It was on this larger scale that the model described by Jung and Taylor (1984) was applied. Cowan and Milthorpe (1968) described the flow in each of the two stages with a separate first-order differential equation. The pair of equations they presented provided the starting point for the analysis which follows in this paper. It will subsequently be shown that there is a dimensionless counterpart of [1] which takes the form

$$\tilde{H} \cdot \Psi_s = 1, \quad [2]$$

where Ψ_s is the dimensionless effective soil water potential over a radial-

axial flow region in which the soil water potential $\tilde{\psi}_s(\sigma)$ is position dependent. Furthermore, there is a weighting function $\tilde{w}(\sigma)$ with the property

$$\int_0^1 \tilde{w}(\sigma) d\sigma = 1,$$

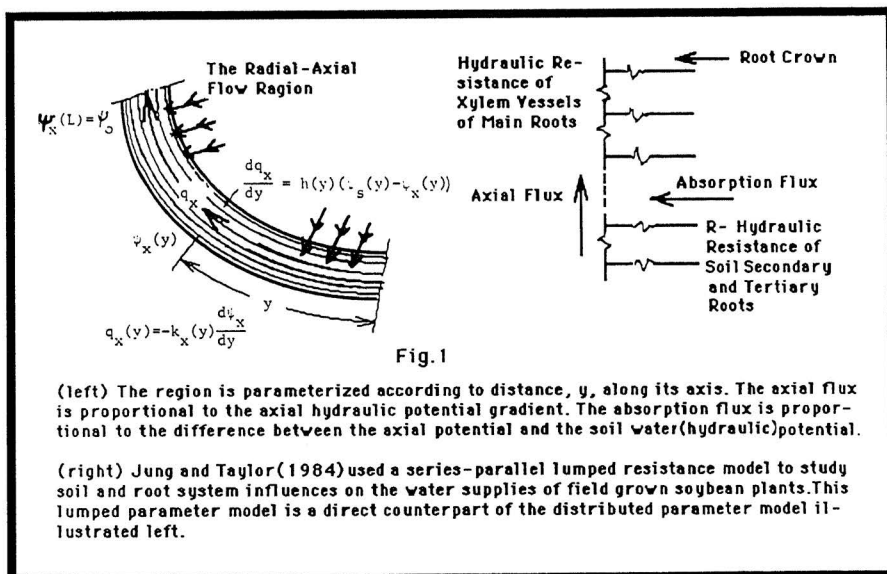
and it will be shown that $\tilde{w}(\sigma)$ generates Ψ_s as

$$\Psi_s = \int_0^1 \tilde{w}(\sigma) \tilde{\psi}_s(\sigma) d\sigma. \quad [3]$$

The Flow System and Boundary Value Problem

An abstraction of the flow region is depicted in Figure 1. The axial component of water flux (q_x) progresses along the interior of the region R' in the direction of the arrows. The distance along the axis, measured from the lower extremity of R' , corresponds to the independent (position) variable, y . The hydraulic potential of water in R' will be referred to as the axial water potential, $\psi_x(y)$, and it varies in an unprescribed manner with y , except at the outflow boundary, $y = L$, where $\psi_x = \psi_0$. The water source, which gives rise to q_x , is soil along the root boundary. The hydraulic potential of water in this region will be referred to as the soil water potential, $\psi_s(y)$, which also depends on position prescribed on the axial flow region, R' . The axial flux in R' is generated by a difference between $\psi_x(y)$ and $\psi_s(y)$. The radial flow of water from R'' to R' augments q_x according to:

$$dq_x/dy = h(y) [\psi_s(y) - \psi_x(y)] \quad [4]$$



The water flux at the inception of the axial region, $y = 0$, is $q_x(0) = 0$, and throughout the region R' , q_x and ψ_x are assumed to be related according to the equation

$$q_x(y) = -k_x(y) \, d\psi_x/dy \quad [5]$$

(From this point on in the discussion, the dependence of k_x , h , ψ_x , and ψ_s on y will be assumed unless otherwise stated, but the dependence will not be explicitly shown.)

Substituting [5] into [4] and rearranging leads to the equation:

$$d(k_x d\psi_x/dy)/dy - h \cdot \psi_x = -h \cdot \psi_s \quad [6]$$

The restriction on the flow at $y = 0$ and the prescribed potential at $y = L$, lead to the boundary conditions:

$$y = 0: \, d\psi_x/dy = 0 \quad [6a]$$

$$y = L: \, \psi_x = \psi_0 \quad [6b]$$

Equation [6], [6a], [6b] constitute a two point boundary value problem representing steady, linear, radial-axial flow. Cowan and Milthorpe (1968) discussed equations equivalent to [4] and [5] in relation to water transport in soil-root systems, and considered the case where h , k_x , and ψ_s are all independent of position. The problem [6] – [6b] is closely related to those described by Carslaw and Jaeger (1959) as "linear flow of heat in the rod," and "cooling fin" problems. The solution to a problem equivalent to [6] – [6b] for the case where h , k_x , and ψ_s are constants appears on pages 141 and 142 of Carslaw and Jaeger (1959) and the solution for the case, which corresponds to a linear k_x and constant ψ_s , appears on page 142. In this latter case the expression for $\psi_x(y)$ would take the form of a linear combination of modified Bessel functions.

We followed the treatment of linear two-point boundary value problems outlined by Stakgold (1967) to arrive at an integral representation of $\psi_x(y)$ where h , k_x , and ψ_s are all position dependent, and from that integral solution, Equations [2] and [3] were obtained. Those two equations together clearly associate $\tilde{w}(\sigma)$ and $\tilde{\Psi}_s(\sigma)$ with the hydraulic conductance model that gives quantitative meaning to the weighted average potential.

Due to its derivation from assumptions related to the flow in soil-root systems, the foregoing statement of the problem in Equations [6] – [6b] has a substantial intuitive basis. However, it is advantageous from the standpoint of reducing the number of solutions required to represent a broad spectrum of physical conditions to remove the dependence of the boundary value problem on the flow path length, L , and the axial potential, ψ_x , at

$y = L$. The following transformation of variables was used to accomplish this:

$$\sigma = y/L \quad [7]$$

$$\tilde{\psi} = (\psi_o - \psi)/\psi_o; \psi_o \neq 0 \quad [8]$$

$$\tilde{q}_x = q_x/q_o; q_o = q_x(L) \quad [9]$$

$$\tilde{k}_x = -k_x \psi_o/q_o L \quad [10]$$

$$\tilde{h} = -h L \psi_o/q_o \quad [11]$$

When substitutions of these variables are made in Equations [6] – [6b], and appropriate rearrangements and simplifications are made, the equivalent dimensionless form of the flow problem is obtained:

$$0 < \sigma < 1: d(\tilde{k}_x d\tilde{\psi}_x/d\sigma)/d\sigma - \tilde{h} \tilde{\psi}_x = -\tilde{h} \tilde{\psi}_s \quad [12]$$

$$\sigma = 0: d\tilde{\psi}_x/d\sigma = 0 \quad [12a]$$

$$\sigma = 1: \tilde{\psi}_x = 0 \quad [12b]$$

Setting the right hand side of Equation [12] equal to zero leads to the corresponding homogeneous differential equation for the system:

$$0 < \sigma < 1: d(\tilde{k}_x d\tilde{\psi}_x/d\sigma) - \tilde{h} \tilde{\psi}_x = 0 \quad [12c]$$

This equation is shown in addition to those required for specification of the flow system, since particular functions, which are obtained as linearly independent solutions to [12c], play a key role in the construction of solutions to the boundary value problem, [12] – [12b].

The dimensionless counterpart of the axial flow Equation [5] is:

$$\tilde{q}_x = -\tilde{k}_x d\tilde{\psi}_x/d\sigma, \quad [13]$$

and the radial flux density Equation [4] is transformed to:

$$d\tilde{q}_x/d\sigma = \tilde{h} (\tilde{\psi}_s - \tilde{\psi}_x) \quad [14]$$

A final note in regard to the transformation of variables [7] – [11], is that in addition to reducing the number of parameters required to represent solutions of the problem, the procedure also leads to a homogeneous condition [12b] (right hand side = 0) corresponding to the outflow boundary. This fact leads to somewhat simpler expressions of the integral solutions of the problem to be presented in the following section.

Green's Function Solution

A Green's function approach (Stakgold, 1967) was used to solve [12] – [12b] in integral form. This procedure leads to an integral expression for the axial potential, and also for the effective soil water potential and the effective system conductance. It will be shown that integrals derived from the Green's function solution provide a direct means for obtaining the first

moment of the weighting function, which generates the effective soil water potential. Before entering the discussion of the solution technique, per se, some background information on the boundary value problem and solution technique will be presented.

According to Stakgold (1967) boundary value problems having the same general form as [12] – [12b] fall into a class of problems for which the solution being sought can be expressed as an integral over the domain of the independent variable, σ . The integrand in the solution is composed of the product of the non-homogeneous term (in the present problem, $-\tilde{h}\tilde{\psi}_s$) from the governing differential equation, and another function, the Green's function, which can be uniquely constructed from linearly independent solutions of the corresponding homogeneous equation. In the present case, the desired solution is of the form:

$$\tilde{\psi}_x(\sigma) = \int_0^1 g(\sigma|\xi) \cdot [-\tilde{h}(\xi) \cdot \tilde{\psi}_s(\xi)] d\xi \quad [15]$$

The Green's function, $g(\sigma|\xi)$, is a special bi-variable function and, as indicated by the integral in [15], is treated as a function of the single variable, ξ , for any fixed value of σ in the interval $0 < \sigma < 1$. When it exists it meets criteria in the following four categories:

- (a) The relationship of g to the homogeneous differential equation: $g(\sigma|\xi)$ must satisfy Equation [12c] for values of $\sigma \neq \xi$.
- (b) The values taken on by g at the system boundaries: it is required that g satisfy homogenous boundary conditions which correspond to the two boundary conditions given for the problem. In the present case, this implies that $g(\sigma|\xi)$ must satisfy [12a] and [12b], since these two equations are homogeneous in their present form.
- (c) Continuity of $g(\sigma|\xi)$ at $\sigma = \xi$: g must be continuous, when considered a function of the single variable, σ , for all values of ξ in the interval $0 < \xi < 1$.
- (d) Jump discontinuity of $g'(\sigma|\xi)$ at $\sigma = \xi$: g' must satisfy the "jump condition"

$$\lim_{\sigma \rightarrow \xi^+} g' - \lim_{\sigma \rightarrow \xi^-} g' = \frac{1}{a_o(\xi)}$$

where $a_o(\xi)$ is the coefficient of the second-order term in the differential equation. In the present problem, $a_o(\xi) = k_x(\xi)$.

We will defer for the present, any further discussion of the specific nature of the Green's function.

In addition to meeting criteria for solution by a Green's function approach, the problem [12] – [12b] can be further classified in a manner which leads to a particularly simple dependence of $g(\sigma|\xi)$ on solutions of the homogeneous Equation [12c]. Second-order linear equations which can be expressed in the form:

$$d(a_0(x)dy/dx)/dx - a_2(x)y = f(x) \quad [16]$$

are said to be formally self-adjoint. Equation [12] qualifies by inspection, provided the appropriate correspondences between variables in [12] and [16] are understood. Moreover, in cases where the boundary conditions for the problem are unmixed, i.e. the first condition depends only on the solution function and its derivatives evaluated at the left end point of the interval ($\sigma = 0$) and the second condition depends only on the function and its derivative evaluated at the right end-point, the system is said to be self-adjoint, provided the governing equation is also formally self-adjoint. Since [12a] depends only on $\tilde{\psi}'_x(0)$ and [12b] depends only on $\tilde{\psi}_x(1)$, the problem [12] – [12b] meets the criteria for self-adjointness.

As a result of the self-adjoint property of the system, the Green's function can be expressed as (Stakgold, 1967):

$$g(\sigma|\xi) = \begin{cases} \tilde{u}_1(\sigma)\tilde{u}_2(\xi)/C, & 0 < \sigma < \xi \\ \tilde{u}_1(\xi)\tilde{u}_2(\sigma)/C, & \xi < \sigma < 1 \end{cases} \quad [17]$$

where \tilde{u}_1 and \tilde{u}_2 satisfy the conditions $u'_1(0) = 0$ and $u_2(1) = 0$. The existence of the functions \tilde{u}_1 and \tilde{u}_2 is guaranteed for self-adjoint systems, provided the coefficient of the second-order term in the governing equation is always non-zero. For the problem at hand, this implies that $\tilde{k}_x(\sigma) \neq 0$ for $0 < \sigma < 1$. This condition is assumed for problems in the present context of soil-root system water transport. Also up to now, only one condition each has been imposed on the functions \tilde{u}_1 and \tilde{u}_2 . It will be shown subsequently that it is advantageous to choose \tilde{u}_1 such that:

$$\tilde{u}_1(1) = 1 \quad [18]$$

and \tilde{u}_2 such that:

$$\tilde{u}'_2(1) = 1 \quad [19]$$

The practical problem of obtaining particular functions, \tilde{u}_1 and \tilde{u}_2 , which satisfy the homogeneous Equation [12c] and the above mentioned boundary value constraints, will be addressed at a later point in the discussion. The constant C in [17] is defined from the coefficient of the second-order term in the governing equation, and the Wronskian, W, of \tilde{u}_1 and \tilde{u}_2 :

$$\begin{aligned} C &= k_x(\sigma) \cdot W(\tilde{u}_1, \tilde{u}_2; \sigma) \\ &= \tilde{k}_x(\sigma) \cdot \begin{vmatrix} \tilde{u}_1(\sigma) & \tilde{u}_2(\sigma) \\ \tilde{u}'_1(\sigma) & \tilde{u}'_2(\sigma) \end{vmatrix} \end{aligned} \quad [20]$$

In general, the product indicated in Equation [20] is a function of σ , but by Abel's formula, C is a constant when the differential equation leading to \tilde{u}_1 and \tilde{u}_2 is of the form [16], i.e. when the equation is formally self-adjoint. Accordingly, Abel's formula, when applied to [20], yields:

$$C = \tilde{k}_x(1) \cdot [\tilde{u}_1(1) \cdot \tilde{u}'_2(1) - \tilde{u}_2(1) \cdot \tilde{u}'_1(1)] = \tilde{k}_x(1). \quad [21]$$

When the constant, C , is substituted into [17], and the resulting expression for $g(\sigma\xi)$ is substituted into Equation [15], the following general representation of the dimensionless axial water potential is obtained:

$$\begin{aligned} \tilde{\psi}_x(\sigma) = [\bar{k}_x(1)]^{-1} \cdot \{ \int_0^\sigma [-\bar{h}(\xi) \tilde{\psi}_s(\xi)] \tilde{u}_1(\xi) \tilde{u}_2(\sigma) d\xi \\ + \int_\sigma^1 [-\bar{h}(\xi) \tilde{\psi}_s(\xi)] \tilde{u}_1(\sigma) \tilde{u}_2(\xi) d\xi \} \end{aligned} \quad [22]$$

Equation [22] implies that at any point in the flow region, the axial potential depends continuously on the spatial distributions of the soil water potential, $\tilde{\psi}_s$, the radial transfer coefficient, \bar{h} , and the axial conductivity, \bar{k}_x . The dependence of $\tilde{\psi}_x$ on \bar{k}_x is not shown explicitly in [22]. Nevertheless, the two functions \tilde{u}_1 and \tilde{u}_2 which appear in the integrands, depend on \bar{k}_x since they both satisfy the homogeneous Equation [12c]. The dependence of $\tilde{\psi}_x$ on the soil water potential upstream from σ is incorporated in the first term in brackets on the right hand side of [22]. This term constitutes a weighted integral of $\tilde{\psi}_s$ over the interval $0 < \xi < \sigma$, with the weighting function proportional to the product of the radial transfer coefficient \bar{h} and the function \tilde{u}_1 , which satisfies the boundary condition [12a] at $\sigma = 0$.

Similarly, the dependence of $\tilde{\psi}_x$ on $\tilde{\psi}_s$ downstream from σ is incorporated in the second integral, which amounts to a weighting of $\tilde{\psi}_s$ in proportion to the product of \bar{h} and the function, \tilde{u}_2 .

One special case of the quantitative dependence of $\tilde{\psi}_x$ on $\tilde{\psi}_s$, that is of particular interest, in the present context, is the use of the Green's function solution to describe the flux at $\sigma = 1$. At this position $\tilde{\psi}_x$ corresponds to the axial potential, $\tilde{\psi}_o$, at the outflow boundary of the flow region. In the original statement of the problem, it was assumed that the value of $\tilde{\psi}_x(1)$ is known. Moreover, [22] does not lead directly to any new information at $\sigma = 1$, since substituting 1 for σ in [22] leads to the boundary condition [12b]. In spite of this, it will now be shown that an expression which relates $\tilde{\psi}_o$ and the flux q_o , to the soil water potential distribution, can be derived from [22].

Before proceeding with the derivation, some terms in Equation [22] will be recombined to arrive at a less cumbersome expression of $\tilde{\psi}_x$. It is also helpful at this point to introduce two additional quantities which will aid in arriving at a simpler form of Equation [22] and which will also be used later in the discussion of system functions.

First, the dimensionless transfer coefficient may be expressed as the product of a normalized function $\bar{h}_n(\sigma)$, and the dimensionless total radial conductance of the region, defined by:

$$\bar{h}_T = \int_0^1 \bar{h}(\sigma) d\sigma \quad [23]$$

Thus we have:

$$\bar{h}(\sigma) = \bar{h}_T \cdot \bar{h}_n(\sigma) \quad [24]$$

Secondly, the total radial to axial conductance ratio for the system will be defined as:

$$\beta^{*2} = \bar{h}_T / \bar{k}_x(1) \quad [25]$$

Returning to the simplification of Equation [22], if $\tilde{u}_2(\sigma)$ is taken outside the first integral on the right hand side, $\tilde{u}_1(\sigma)$ is taken outside the second integral, and the defining Equations [24], for \bar{h}_T , and [25], for β^{*2} , are used, then:

$$\tilde{\psi}_x(\sigma) = -\beta^{*2} \{ \tilde{u}_2(\sigma) \cdot \Phi_1(\sigma) + \tilde{u}_1(\sigma) \cdot \Phi_2(\sigma) \} \quad [26]$$

where

$$\Phi_1(\sigma) = \int_0^\sigma \bar{h}_n(\xi) \tilde{u}_1(\xi) \tilde{\psi}_s(\xi) d\xi, \quad [27]$$

and

$$\Phi_2(\sigma) = \int_\sigma^1 \bar{h}_n(\xi) \tilde{u}_2(\xi) \tilde{\psi}_s(\xi) d\xi \quad [28]$$

Differentiating [27] and [28] with respect to σ leads to the following expressions for the derivatives of Φ_1 and Φ_2 :

$$\Phi_1'(\sigma) = \bar{h}_n(\sigma) \cdot \tilde{u}_1(\sigma) \cdot \tilde{\psi}_s(\sigma) \quad [29]$$

$$\Phi_2'(\sigma) = -\bar{h}_n(\sigma) \cdot \tilde{u}_2(\sigma) \cdot \tilde{\psi}_s(\sigma). \quad [30]$$

Finally, multiplying both sides of [29] by $\tilde{u}_2(\sigma)$ and both sides of [30] by $\tilde{u}_1(\sigma)$ we have, upon addition of the resulting terms:

$$\tilde{u}_2(\sigma) \cdot \Phi_1'(\sigma) + \tilde{u}_1(\sigma) \cdot \Phi_2'(\sigma) = 0.$$

Differentiating [26] with respect to σ , and making use of the above equation, the following expression is obtained for the derivative of the dimensionless axial water potential:

$$\psi_x'(\sigma) = -\beta^{*2} \{ \tilde{u}_2'(\sigma) \cdot \Phi_1(\sigma) + \tilde{u}_1'(\sigma) \cdot \Phi_2(\sigma) \} \quad [31]$$

System Flow Equation

The dimensionless axial flux may be obtained by multiplying both sides of Equation [31] by $-\tilde{k}_x(\sigma)$. The following dimensionless system flow equation is obtained by evaluating the resulting expression for $\sigma = 1$. Since $\tilde{q}_x(1) = q_x(L)/q_o = 1$, we have:

$$-\tilde{k}_x(1) \tilde{\psi}'_x(1) = 1 \quad [32a]$$

$$\tilde{k}_x(1) \cdot \beta^{*2} \cdot \Phi_1(1) = 1, \quad [32b]$$

or

$$\tilde{h}_T \cdot \Phi_1(1) = 1 \quad [32c]$$

Equation [32b] follows from [31], when it is recognized that: $\tilde{u}'_2(1) = 1$ and $\Phi_2(1) = 0$. Equation [32c] follows from [32b] and the definition of β^{*2} in Equation [25].

The above equations represent a fundamental relationship among the variables \tilde{h} , \tilde{k}_x , and $\tilde{\psi}_s$ over the flow region: $0 < \sigma < 1$. It will be shown that they lead to expressions of the effective soil water potential and effective system conductance for conditions of steady, radial-axial flow. Before proceeding with the derivations of the system functions, we make the following observation regarding the use of Equation [32] to obtain information about the curvature of the graph of ψ_x and about the possibility of reverse flows from the region R' into the region R'' of Figure 1. Certain combinations of \tilde{h} , \tilde{k}_x , and $\tilde{\psi}_s$ lead to $\tilde{\psi}_x$ distributions where the derivative $\tilde{\psi}'_x(\sigma)$, and hence also the flux, \tilde{q}_x , is equal to zero for some particular value σ^* in the interval, $0 < \sigma^* < 1$. Values of σ where $\tilde{\psi}'_x = 0$ are critical values, and the condition for a critical value of σ , in terms of the Equation [31] for $\tilde{\psi}'_x(\sigma)$ is:

$$\tilde{u}'_2(\sigma^*) \Phi_1(\sigma^*) + \tilde{u}'_1(\sigma^*) \Phi_2(\sigma^*) = 0 \quad [33]$$

At points along the flow axis which correspond to critical values, the function $\tilde{\psi}_x$ will exhibit a maximum or a minimum value. In cases where \tilde{h} , \tilde{k}_x , and $\tilde{\psi}_s$ have analytical representations in terms of closed form functions, criteria can be sought on the parameters of the representing functions, which lead to critical values of σ , and expressions for σ^* can be sought in terms of the function parameters. Hereafter, critical values will be referred to as flux reversal points to more clearly associate them with the flow problem under consideration.

The Effective Potential And Effective Conductance

At the outset it was stated that one of the objectives is to arrive at descriptions of the effective soil water potential and effective system conductance within a distributed parameter framework. Accordingly we

will now show that the flow Equation [32] leads directly to those quantities for the system under consideration. Returning to [32c] we have

$$\tilde{h}_T \cdot \Phi_1(1) = 1 \quad [32c]$$

The dimensionless effective soil water potential for the system is,

$$\tilde{\psi}_s = \Phi_1(1)/D_{h,k}, \text{ where } D_{h,k} = \int_0^1 \tilde{h}_n(\sigma)\tilde{u}_1(\sigma)d\sigma,$$

so Equation [32c] becomes

$$\tilde{H} \cdot \tilde{\psi}_s = 1, \quad [33]$$

where

$$\tilde{H} = \tilde{h}_T \cdot \int_0^1 \tilde{h}_n(\sigma) u_1(\sigma) d\sigma = \tilde{h}_T \cdot D_{h,k}. \quad [34]$$

Accordingly, $\tilde{\psi}_s$ is a weighted average of the dimensionless soil water potential over the flow region,

$$\tilde{\psi}_s = \int_0^1 \tilde{w}(\sigma) \tilde{\psi}_s(\sigma) d\sigma, \quad [35]$$

where

$$\tilde{w}(\sigma) = \tilde{h}_n(\sigma) \cdot \tilde{u}_1(\sigma)/D_{h,k} \quad [36]$$

The weighting function, $\tilde{w}(\sigma)$, has the property:

$$\int_0^1 \tilde{w}(\sigma) d\sigma = 1. \quad [37]$$

It can be shown that the back transformations of \tilde{H} and $\tilde{\psi}_s$ in the original dimensional system are H and ψ_s which satisfy the flow equation

$$q_o = H (\psi_s - \psi_o).$$

For this reason \tilde{H} will be referred to as the dimensionless system conductance and $\tilde{\psi}_s$ will be referred to as the dimensionless effective soil water potential with weighting function $\tilde{w}(\sigma)$.

Equation [36] shows that the magnitude of \tilde{w} at a given position depends on the magnitudes of the normalized transfer coefficient distribution, \tilde{h}_n , and the function \tilde{u}_1 , at the same position. It can be shown (Personal communication with Calvin Ahlbrandt of the Department of Mathematics, UMC) that \tilde{u}_1 is a non-decreasing function, and from Equation [18], its maximum value is one at $\sigma = 1$. Therefore, the weighting which \tilde{w} imparts to the soil water potential at a given distance away from the outflow boundary is proportional to the value of the transfer coefficient distribution at that position, and the weighting is increasingly diminished with increasing distance away from the outflow boundary. The magnitude of $D_{h,k}$ in turn depends on the product of \tilde{h}_n and \tilde{u}_1 over the entire flow region and therefore reflects the diminution of water potential weighting associated with the greater axial resistance encountered by water entering the axial pathway at points further upstream.

Equation [32] provides a partial basis for calculating the system functions from $\tilde{\psi}_s(\sigma)$, $\tilde{h}(\sigma)$ and $\tilde{k}_x(\sigma)$. By integrating both sides of the

auxiliary flow Equation [12c] between limits of $\sigma = 0$ and $\sigma = 1$, it is possible to obtain some additional useful formulas relating H and $D_{h,k}$ to $\tilde{u}'_1(1)$. Integrating both terms in [6c] leads to:

$$\int_0^1 [d(\tilde{k}_x(\sigma) \cdot d\tilde{u}_1/d\sigma)/d\sigma]d\sigma = \int_0^1 \tilde{h}(\sigma)\tilde{u}_1(\sigma)d\sigma. \quad [38]$$

Noting the definitions of \tilde{H} and $D_{h,k}$, [Eq. 34] and using the fact that $\tilde{u}'_1(0) = 0$, the above integration leads to

$$\tilde{k}_x(1) \cdot \tilde{u}'_1(1) = \tilde{H}, \quad [39]$$

or alternatively,

$$\tilde{u}'_1(1)/\beta^{*2} = D_{h,k}. \quad [40]$$

Equations [39] and [40], in conjunction with Equations [32a] – [32c], can be used as a basis for a numerical procedure for calculating $\tilde{\psi}_s$, $D_{h,k}$ and \tilde{H} .

Back-Transformation Equations

The derived dimensionless system functions can be back-transformed into the system which corresponds directly to Figure 1 and to the original statement of the boundary value problem, Equations [6] – [6b]. The convention which has been followed up to now, regarding the use of symbols in the dimensionless versus original systems, is to represent a variable in the dimensionless system using the corresponding symbol from the original system, capped with a $\tilde{}$. The same convention will be adhered to in the back-transformation scheme. Mathematical details of the back-transformation are omitted.

Total Radial Conductance

$$h_T = \int_0^L h(y)dy = -\frac{q_o}{\psi_o} \cdot \tilde{h}_T \quad [41]$$

Normalized Transfer Coefficient

$$h_n(y) = h(y)/h_T = \frac{1}{L} \frac{h(\sigma)}{h_T} = \tilde{h}_n(\sigma)/L \quad [42]$$

Axial Conductivity

$$k_x(y) = -\frac{q_o L}{\psi_o} \cdot \tilde{k}_x(\sigma) \quad [43]$$

Radial-Axial Conductance

$$H = h_T \cdot D_{h,k} = -\frac{q_o}{\psi_o} \tilde{h}_T \cdot D_{h,k} = -\frac{q_o}{\psi_o} \cdot \tilde{H} \quad [44]$$

Effective Soil Water Potential

$$\psi_s = \psi_o (1 - \tilde{\psi}_s) \quad [45]$$

System Flow Equation

$$\tilde{H} \cdot \tilde{\psi}_s = 1 \quad [46a]$$

$$-\frac{\Psi_o}{q_o} H \cdot \frac{\Psi_o - \psi_s}{\psi_o} = 1 \quad [46b]$$

$$H \cdot (\psi_s - \psi_o) = q_o \quad [46c]$$

In a specific application of the theory, it might be desired to calculate the flux, q_o ; the effective radial-axial conductance, H ; and the effective soil water potential Ψ_s , which arise in association with a specified value of the outflow boundary potential, ψ_o , and specified $k_x(y)$, $h(y)$, and $\psi_s(y)$. A procedure is outlined below for doing this. The outline assumes availability of the above mentioned (known) quantities and also assumes either a numerical or analytical procedure is available for calculating $\tilde{\psi}_x(\sigma)$, $\tilde{\psi}'_x(\sigma)$, $\tilde{u}_1(\sigma)$, and $\tilde{u}'_1(\sigma)$. A numerical procedure for computing these quantities for the special case $k_x(\sigma) = \tilde{k}_x^*(\text{constant})$ has been tested. The procedure outlined below for the computation of q_o , and back-transformation of the system functions also assumes \tilde{k}_x constant.

Step 1:

Starting with k_x^* , $h(y)$, and $\psi_s(y)$ in the dimensional system, calculate the dimensionless conductance ratio, β^{*2} as follows:

(a) Calculate $h_T = \int_0^L h(y) dy$

(b) Calculate $\beta^{*2} = L \cdot h_T / k_x^*$.

Step 2:

Calculate $\tilde{h}_n(\sigma) = L h(\sigma \cdot L) / h_T$ $0 \leq \sigma \leq 1$

Step 3:

Calculate $\tilde{\psi}_s(\sigma) = (\psi_o - \psi_s(\sigma \cdot L)) / \psi_o$ $0 \leq \sigma \leq 1$

Step 4:

Solve the $\tilde{\psi}_x$ flow problem and the \tilde{u}_1 (auxiliary flow) problem using an available procedure. An approach that has been very satisfactory utilizes a "shooting technique" (Carnahan et al., 1969) which is based on a fourth order Runge-Kutta procedure. The solution of these boundary value problems produces values of $\tilde{\psi}'_x(1)$ and $\tilde{u}'_1(1)$.

Step 5:

Calculate the value of the system distribution constant (see Equation [40])

$$D_{h,k} = \tilde{u}'_1(1) / \beta^{*2}$$

Step 6:

Calculate the dimensionless effective soil water potential. For this step we make use of Equations [32a] – [32b], and the definition of $\tilde{\psi}_s$:

$$\Psi_s = \tilde{\psi}'_x(1) / \beta^{*2} \cdot D_{h,k}$$

Step 7:

Calculate the dimensional effective system conductance

$$H = h_T \cdot D_{h,k}$$

Step 8:

Calculate the dimensional effective water potential

$$\Psi_s = \psi_o(1 - \Psi_s)$$

Step 9:

Calculate the dimensional flux q_o :

$$q_o = H \cdot (\Psi_s - \psi_o).$$

The System For Constant \bar{h} And \bar{k}_x

The preceding analysis led to the dimensionless conductance Equation [2] which back-transforms into a similar conductance equation in the dimensional system. The back-transformation of Equation [2] is mathematically equivalent to Equation [1] for non-zero values of H , the dimensionless system conductance. The conductance properties of the system depend only on the dimensionless axial conductivity, $\bar{k}_x(\sigma)$, and the dimensionless radial transfer coefficient $\bar{h}(\sigma)$. The interactive behavior of these two hydraulic properties in determining the overall effective conductance for transport of water from the soil (region R'' in Figure 1), to the outflow boundary of the axial flow region, is determined by the homogeneous differential Equation [12c]. Two linearly independent solutions of this equation are $\bar{u}_1(\sigma)$ and $\bar{u}_2(\sigma)$, which were uniquely selected to satisfy particular boundary conditions. The function $\bar{u}_1(\sigma)$ can be interpreted as the hypothetical potential distribution corresponding to a potential of $\psi_x = 0$, at the outflow boundary of the dimensional system, and a uniform soil water potential, $\psi_s(y) = \psi_o$.

The effective conductance properties of the system are summarized in Equation [44], as the product of the system distribution constant $D_{h,k}$ and the total radial conductance, h_T . This product is the effective conductance in the original system:

$$H = h_T \cdot D_{h,k}. \quad [44]$$

The maximum value of $D_{h,k}$ is 1, so Equation [44] expresses the effective system conductance as a fraction of the total radial conductance. In turn the total radial conductance serves as the limiting value of H . In fact, it can be shown that, when $k_x(y)$ is a constant,

$$\lim_{\beta^{*2} \rightarrow 0} \bar{H} = \bar{h}_T.$$

That limit is not expected to be precisely achieved in real systems, but small β^{*2} reflects a situation where the chief limitations to flow are in the radial, rather than in the axial, pathway.

In the dimensional system, the value of the soil water potential which is effective in driving the flow, in the sense of ψ_1 in Equation [1], is Ψ_s , the back-transformed counterpart of Ψ_s . According to Equations [35] and [36], this effective potential depends on two categories of factors. It depends on the soil water potential distribution, $\tilde{\psi}_s(\sigma)$, and it depends on the conductance properties of the soil-root system, as those properties are manifested in the weighting function

$$\tilde{w}(\sigma) = \tilde{h}_n(\sigma)\tilde{u}_1(\sigma)/D_{h,k}$$

This is reasonable.

The preceding observations were borne out in two particular studies of the system behavior. In one of these, closed-form representations of the functions discussed in the preceding analysis were obtained for the special case of constant axial conductivity, constant radial transfer coefficient, and a linear soil water potential distribution. In the second study, a qualitative analysis was carried out for the special case of constant axial conductivity and linear soil water potential distribution. The second study required a numerical procedure, and it was based on graphs that were generated using a range of β^{*2} and seven different transfer coefficient distribution functions.

Table 2 contains a list of closed form expressions for the case $\tilde{h}(\sigma) = h^*$, $\tilde{k}_x(\sigma) = k_x^*$, and $\tilde{\psi}_s(\sigma) = \sigma$. The functions $\tilde{u}_1(\sigma)$ and $\tilde{u}_2(\sigma)$ are hyperbolic cosine and hyperbolic sine functions, respectively, and since $\tilde{\psi}_x(\sigma)$, $\tilde{q}_x(\sigma)$, $\tilde{w}(\sigma)$, $D_{h,k}$, \tilde{H} , and $\tilde{\Psi}_s$ depend on those two solutions of the homogeneous equation, their expressions also contain hyperbolic functions. Figures 2(a), 2(b), and 2(c) show the behavior of $\tilde{u}_1(\sigma)$, $\tilde{w}(\sigma)$, $\tilde{\psi}_x(\sigma)$, and $\tilde{q}_x(\sigma)$ for $\beta^{*2} = 0.1, 1.0, \text{ and } 10.0$, respectively. The graph of $\tilde{\psi}_x(\sigma)$ in Figure 2(a), where $\beta^{*2} = 0.1$, approaches the uniformity that has sometimes been assumed in models of soil-root system water transport.

Table 2
Constants and System Functions
for $\tilde{h}(\sigma) = \tilde{h}^*$ and $\tilde{k}_x(\sigma) = \tilde{k}^*$

- (1) Transfer coefficient distribution

$$\tilde{h}_n(\sigma) = 1$$

- (2) Total radial conductance

$$\tilde{h}_T = \tilde{h}^*$$

- (3) Total radial to axial conductance ratio

$$\beta^{*2} = \tilde{h}^*/\tilde{k}^*$$

- (4) Solution to the auxiliary boundary value problem

$$\tilde{u}_1(\sigma) = \cosh(\beta^*\sigma)/\cosh \beta^*$$

- (5) Solution to the auxiliary initial value problem

$$\tilde{u}_2(\sigma) = \beta^{*-1} \sinh[\beta^*(\sigma - 1)]$$

- (6) Distribution constant

$$D_{h,k} = \beta^{*-1} \tanh \beta^*$$

- (7) First integral term of the Green's function solution

$$\Phi_1(\sigma) = \int_0^\sigma \cosh(\beta^*\xi) \tilde{\psi}_s(\xi) d\xi / \cosh \beta^*$$

- (8) Second integral term of the Green's function solution

$$\Phi_2(\sigma) = \beta^{*-1} \int_\sigma^1 \sinh[\beta^*(\xi - 1)] \cdot \tilde{\psi}_s(\xi) d\xi$$

- (9) Effective system conductance

$$\tilde{H} = (\tilde{h}^*\tilde{k}^*)^{1/2} \tanh \beta^*$$

- (10) Effective soil water potential

$$\Psi_s = \beta^* [\int_0^1 \cosh(\beta^*\xi) \tilde{\psi}_s(\xi) d\xi] / \sinh \beta^*$$

- (11) Weighting function for the effective water potential

$$\tilde{w}(\sigma) = \beta^* \cosh(\beta^*\sigma) / \sinh \beta^*$$

**Equations (12) – (18) Correspond to the Linear
Soil Water Potential Distribution $\psi_s(\sigma) = \sigma$**

- (12) Effective soil water potential and first moment of the weighting function distribution

$$\Psi_s = \bar{\sigma}_w = 1 + \beta^{*-1} (\operatorname{csch} \beta^* - \operatorname{ctnh} \beta^*)$$

- (13) First integral term of the Green's function solution

$$\Phi_1(\sigma) = \beta^{*-2} [\beta^* \sigma \sinh(\beta^* \sigma) - \cosh(\beta^* \sigma) + 1] / \cosh \beta^*$$

- (14) Second integral term of the Green's function solution

$$\Phi_2(\sigma) = \beta^{*-2} [1 - \sigma \cosh[\beta^*(1 - \sigma)] - \sinh[\beta^*(1 - \sigma)]] / \beta^*$$

- (15) Axial water potential

$$\tilde{\Psi}_x(\sigma) = \sigma + [\beta^{*-1} \sinh[\beta^*(1 - \sigma)] - \cosh \beta^* \sigma] / \cosh \beta^*$$

- (16) Derivative of axial water potential

$$\tilde{\Psi}'_x(\sigma) = 1 - \{\beta^* \sinh \beta^* \sigma + \cosh[\beta^*(1 - \sigma)]\} / \cosh \beta^*$$

- (17) Equation whose root is the flux-reversal point

$$\beta^* \sinh(\beta^* \sigma^*) + \cosh[\beta^*(1 - \sigma^*)] = \cosh \beta^*$$

It is evident (Figures 2(a), 2(b) and 2(c)) that an increase in β^{*2} leads to a greater departure of $\tilde{u}_1(\sigma)$ from unity and a corresponding steepening of the weighting function $\tilde{w}(\sigma)$. Such an increase in β^{*2} would accompany an increase in the length of the axial pathway or an increase in the ratio of the radial transfer coefficient to the axial conductivity. Higher values of β^{*2} also lead to steeper axial potential gradients and a shift of the water flow pattern determined by the linear soil water potential distribution. For the given $\tilde{\psi}_s(\sigma)$, the axial potential is lowered enough at $\beta^{*2} = 1.0$ to result in noticeable leakage of water from the axial region into the soil. The leakage is severe over half the axial region at $\beta^{*2} = 10.0$.

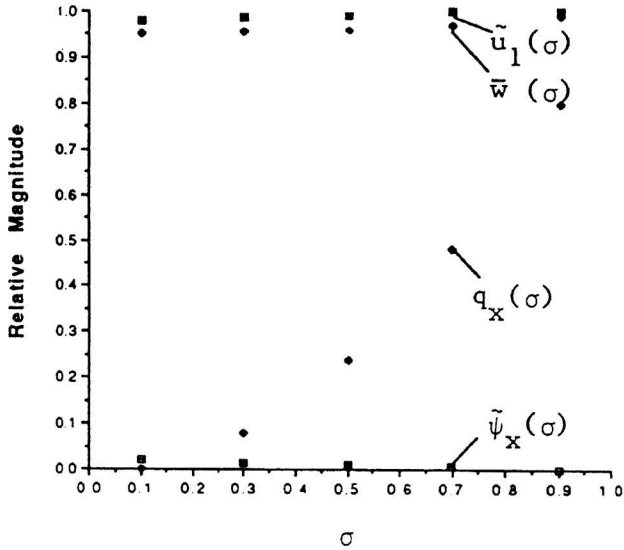


Fig.2(a) Dimensionless flow variables plotted as functions of σ for $\tilde{\psi}_s(\sigma) = \sigma$ and $\beta^{*2} = 0.1$

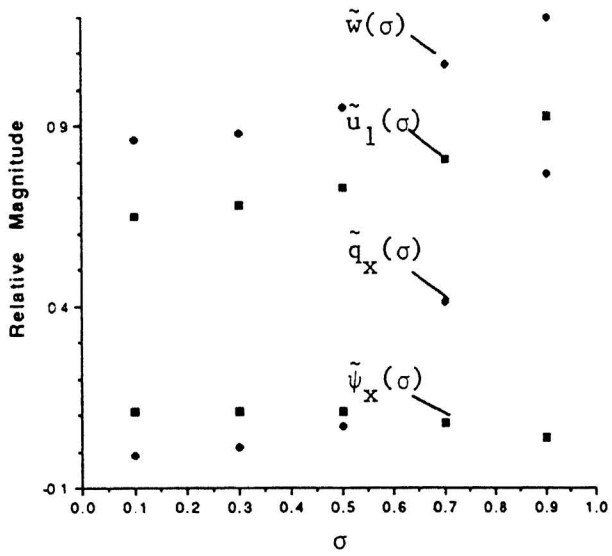


Fig.2(b) Dimensionless flow variables plotted as functions of σ for $\psi_S(\sigma) = \sigma$ and $\beta^*^2 = 1.0$

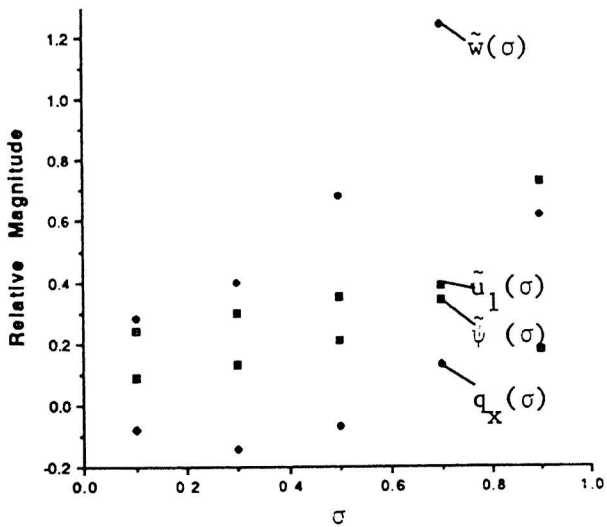


Fig.2(c) Dimensionless flow variables plotted as functions of σ for $\psi_S(\sigma) = \sigma$ and $\beta^* = 10.0$

Figure 3 contains graphs of $D_{h,k}$ and Ψ_s for $\bar{h} = \bar{h}^*$, $\bar{k}_x = \bar{k}_x^* \bar{\psi}_s(\sigma) = \sigma$. As β^{*2} increases from 0.1 to 1.0 the modest decrease in $D_{h,k}$ from 0.97 to 0.77 reflects the proportionate decrease in the system conductance over this range of β^{*2} . There is a larger proportionate decrease in $D_{h,k}$, from 0.79 to 0.32 as β^{*2} increases from 1.0 to 10.0. The dimensionless effective soil water potential increases from 0.50 to 0.54 as β^{*2} increases from 0.1 to 1.0, and Ψ_s is approximately 0.71 for $\beta^{*2} = 10.0$.

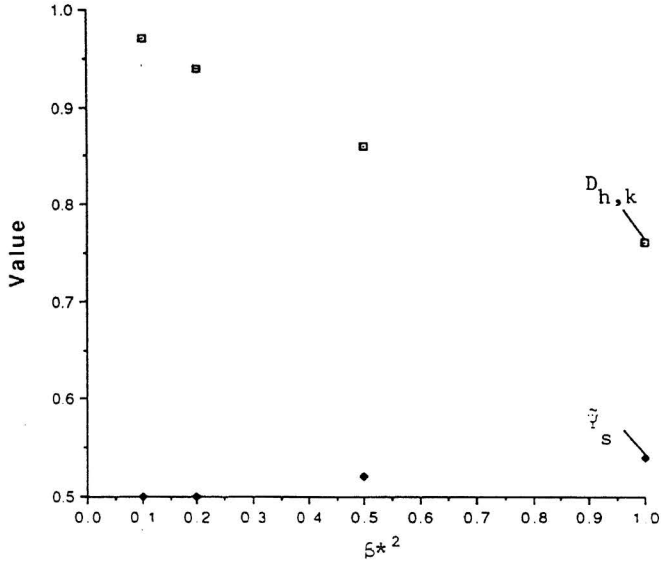


Fig.3(a) Effective soil water potential and the distribution constant as the functions of β^{*2} , constant h,k.

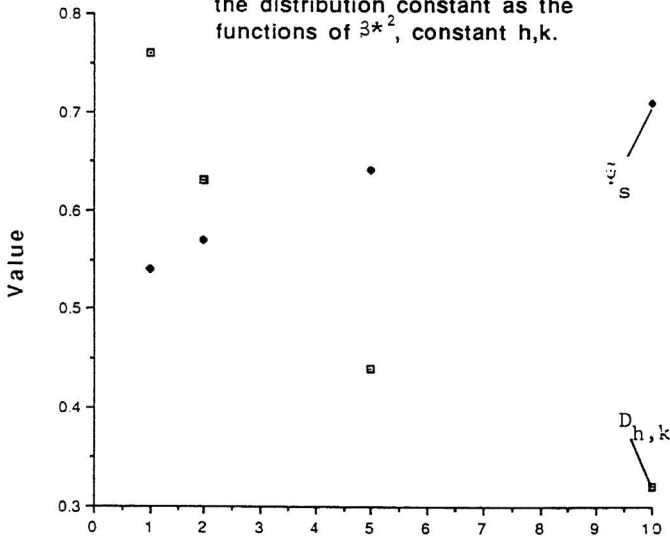


Fig.3(b) Effective soil water potential and the distribution constant as the functions of β^{*2} , constant h,k.

Concluding Remarks

This study was undertaken in the hope of better understanding, and better using, the hydraulic resistance Equation [1] as a model of water transport in soil-root systems. Such a model is needed for interpreting soil and root system influences on plant water supplies.

The structure of Equation [1] carries implications of linearity and steady-flow that are not rigorously characteristic of the system being modeled. It also implies a homogeneity of component water potentials with regard to their interaction with the resistance, R , in determining the flux, q . This latter implication seems unlikely to carry over when both the hydraulic potential and the osmotic potential are operative in the water transport. Various strategies have been used for adapting the equation empirically to experimental conditions (Klepper and Taylor, 1978). The present study focused on the representation of a spatially variable soil water potential, as a single effective potential, in the sense of ψ_1 of Equation [1].

The very linearity, which has been cited as a weakness of the equation, gives it considerable power in coping with complex flow geometries, and with the position dependent soil water potentials that characterize these systems. Fluxes and potentials can be partitioned among various components of the system in a manner that is readily interpretable, so far as the relationship between component resistances and the overall system resistance is concerned. In this study attention was restricted to the soil-root subsystem of the soil-plant system.

Water flow in soil-root systems is characterized by a radial-axial configuration. Cowan and Milthorpe (1968) assumed that the rate of water flow into a root system is proportional to the difference between the xylem water potential and the soil water potential. They further assumed that the axial water flux is proportional to the axial potential gradient and also that the gradient itself is parallel to the root axis. Their two equations provided the basis for the two-point boundary value problem upon which the present study was focused. A Green's function technique (Stakgold, 1967) was used to obtain an integral expression of the axial potential, as a function of position along the axial pathway, for conditions of steady-flow and a uniformly zero osmotic potential. The integral solution of the boundary value problem [12] – [12b] was differentiated to obtain an expression for the axial flux at the system outflow boundary. The resulting hydraulic conductance equation [2] is equivalent to the hydraulic resistance equation [1]. The overall impact of the two position dependent system hydraulic properties $h(y)$ and $k_x(y)$, on the flux at the outflow boundary, are summarized in the value of the effective system conductance, H . The representative value of the soil water potential, which drives the flow in the sense of ψ_1 , of equation [1], is a weighted average, Ψ_s , of the position-dependent soil water potential, over the axial flow region. Its value depends on the two position dependent hydraulic properties of the soil-root system, as well as on the soil water potential.

The series-parallel lumped resistance model used by Jung and Taylor (1984) is analogous to the distributed parameter model of the present study. They used the model to analyze soil and plant water phenomena associated with the root systems of field-grown soybean plants. We decided to carry out the analysis without reference to the particular manner in which the axial conductivity and the radial transfer coefficient appear to depend on soil and root system biophysical variables. It is hoped that the analysis given will prove more useful to investigators in the form presented, with rather explicit reference to the underlying flow assumptions.

The problem and its solution apply in a general sense to the radial-axial flow geometry of soil-root systems, and is perhaps useful on more than one scale (Cowan and Milthorpe, 1968). The same basic geometry applies to the flow which occurs in individual roots, and to the flow which occurs in whole root systems. However, the specific nature of the dependence of the two soil-root system hydraulic variables on particular physiological or physical properties of the system is expected to differ considerably for the different scales of application. For example, Jung and Taylor (1984) incorporated the total resistances offered by secondary and tertiary roots in addition to external soil resistances, into their radial resistance term. The inverse of that term is roughly analogous to the radial transfer coefficient of the model considered here. On the smaller scale, absorption of water by a single root would only encounter the resistance to flow offered by the tissues of that root, the soil-root interface, and the surrounding soil. On either scale, to the extent that significant potential gradients accompany water flow in the soil, during absorption, the value of the transfer coefficient may reflect both geometric and hydraulic characteristics of the soil water flow pattern.

The specific nature of the water potential distribution in the axial pathway is an open question, and it is hoped that this model will be of help to those who are devising strategies and techniques for addressing this question. Many scientists believe the total difference, between observed values of plant and soil water potentials, is dominated by root tissues in the radial pathway. This belief seems to rest heavily on estimates of the soil resistance that are made from measured soil hydraulic conductivities, together with estimates of the axial resistance that are based on Poiseuille's law (Meyer et al., 1978; Jung and Taylor, 1984). These latter estimates have been supported to some extent by resistances measured on excised roots (Kozinka, 1981).

Observations of Klepper and Taylor (1978) and Klepper (1983) led us to the conclusion that it is too early to discount the possible importance of axial hydraulic resistances to overall potential differences between soil and plant.

Two issues are highlighted in the radial-axial flow problem and its application to soil-root system water transport. One surrounds the geometry of the flow and of the related axial and soil water potential fields. The other is the effective soil water potential concept. These two issues are

intimately interrelated, and both involve particular geometric and hydraulic properties of the system.

The flow modeled here is convergent toward the root system interior, at any given position along the axial pathway, and it is also convergent over the axial pathway toward the outflow boundary. This modeled geometry is in abstract agreement with what actually happens in these systems. However, the predicted variation in the axial potential with position along the axial pathway is the direct result of two assumptions. One of these is that the axial flux is proportional to the axial potential gradient. The other is that the axial potential gradient is in turn parallel to the root axis at each position along the pathway. This second assumption is easy to overlook as an assumption. We have thereby built into the model exactly one mechanism for changes in potential to accompany the axial flow. In plant root systems, xylem vessels occur in bundles and water exchange can occur among the vessels of these bundles (Klepper, 1983). How relatively important these transverse flows are to the migration of water over longer distances in the root interior, and the extent to which significant potential drops accompany the transverse flows, doesn't seem to be clearly established. Apparently, according to Klepper (1983), there is little resistance to exchange between two vessels in a single bundle. Nevertheless, it is important to bear in mind that the orientation of the axial potential gradient along the root axis is an assumption. If in a given system, the potential variations associated with transverse flows were to dominate, both the potential distribution interior to the root system, and the nature of the controlling hydraulic variable for the axial pathway, would differ considerably from those of the present model.

Another geometric aspect of the problem concerns the prescription of the soil water potential as a function of distance along the axial pathway. The soil water potential is most often mapped in a reference frame that is fixed relative to the soil surface. This is particularly convenient since the vertical component of a soil water flux often dominates it. On the other hand the model described here requires a frame of reference that depends on the geometry of the root system. Specifically, the position of a point in the root zone must be mapped according to its axial distance from the root crown, and also according to its location in the soil water potential measurement frame, in order to determine $\psi_s(y)$ for the boundary data. Although no general procedure seems to be available, it is of interest to note how this correspondence was accomplished in the study made by Jung and Taylor (1984).

Their investigation focused on the water relations of field grown soybeans and measurements of the plant water potential were made in conjunction with the soil water potential distribution and soil water content distribution in the root zone. They analyzed the flow in both the soil and the plant in one spatial dimension, with the axial flow in the soybean plants occurring vertically upward along the main root axis, and encountering a position dependent axial resistance, R_x . Their model treated the soil

water potential and soil water content distributions as horizontally uniform. The radial flow from a soil layer of thickness ΔZ , and centered at depth Z , was assumed to encounter a radial resistance R , as it moved from the soil through tertiary and secondary roots. In effect the lateral roots in each soil layer were treated as a uniformly distributed, diffuse absorbing mat. With the assumed horizontal uniformity of the soil water potential, there was a functional dependence of ψ_s on the depth, Z , in the soil. However, since the main root, where the axial pathway was located was oriented vertically, distance along the axial pathway in their system was also in one-to-one correspondence with the soil depth. Consequently, the soil water potential could be established as a function of position along the axial pathway. A similar correspondence between the axial position variable, and the soil water potential of a soil-based reference frame, might be established for more complex axial pathway geometries, if that becomes necessary.

The effective soil water potential concept is important to our further understanding and characterization of plant water supplies (Gardner, 1964; Gardner, 1968; Jordan and Ritchie, 1971). For the present, quantitative expressions and interpretations of the concept appear to be firmly anchored in hydraulic resistance equations [1], or their conductance counterparts [2]. As the specific nature of flow regulating properties of soil-root systems becomes more certain, it will perhaps be possible to generate pathway specific equations and variables with greater certainty. For the present, there is no unique, or apparently even widely accepted approach to computing a representative value of the spatially variable soil water potential distribution. However, if a given computational framework is to be useful, the distribution of the weighting function which generates ψ_s should be consistent with observed spatially variable quantities of the soil-root system. For the system considered here, $\tilde{w}(\sigma)$ depends interactively on the radial transfer coefficient distribution and the axial conductivity. These in turn depend on the path connecting a point of absorption with the root crown. But this is not to say that only pathway specific equations are legitimate, to the exclusion of non-pathway specific equations.

Wenkert (1983) pointed out the validity of hydraulic resistance equations, in a phenomenological sense. If, in a one-dimensional system, $S(Z)$ represents the depth dependent root water absorption rate, and it is assumed that

$$S(Z) = \hat{h}(Z) [\psi_s(Z) - \psi_2], \quad [47]$$

where ψ_2 is a representative value of the canopy water potential, the absorption rate for the root system as a whole is

$$A = \int_0^D S(Z)dZ = \int_0^D \hat{h}(Z)[\psi_s(Z) - \psi_2] dZ$$

or

$$A = \hat{H} \cdot [\hat{\Psi}_s - \psi_2], \quad [48]$$

where

$$\hat{H} = \int_0^D \hat{h}(Z)dZ.$$

In a system where soil hydraulic properties have been determined and the volumetric water content and soil water potential have been determined as functions of depth and time, $S(Z)$ can be determined from the unsaturated soil moisture flow theory (van Bavel et al., 1967). All that remains to calculate $\hat{h}(Z)$ is ψ_2 , so \hat{H} and $\hat{\Psi}_s$ can be determined consistent with an observed root water absorption pattern, but independent of hydraulic properties of the root system, per se. Obtaining consistency between phenomenological, non-pathway specific, values of $\hat{\Psi}_s$ and \hat{H} , and particular pathway specific counterparts, appears to be a worthwhile goal for future experimental applications of the theory.

References

- Blanchar, R. W., C. R. Edmonds, and J. M. Bradford. 1978. Root growth in cores formed from fragipan and B2 horizons of Hobson soil. *Soil Sci. Soc. Am. J.* 42(3):437-440.
- Bradford, J. M. and R. W. Blanchar. 1977. Profile modification of a fragiudalf to increase crop production. *Soil Sci. Soc. Am. J.* 41:127-131.
- Bradford, J. M. and R. W. Blanchar. 1980. The effect of profile modification of a fragiudalf on water extraction and growth by grain sorghum. *Soil Sci. Soc. Am. J.* 44(2):374-378.
- Carnahan, B., H. A. Luther, and J. O. Wilkes. 1969. *Applied numerical methods*. John Wiley and Sons, N.Y.
- Carslaw, H. S. and J. C. Jaeger. 1959. *Conduction of heat in solids*, 2nd Ed. Oxford University Press, London.
- Corey, A. T. and A. Klute. 1985. Application of the potential concept to soil water equilibrium and transport. *Soil Sci. Soc. Am. J.* 49:3-11.
- Cowan, I. R. 1965. Transport of water in the soil-plant-atmosphere system. *J. Appl. Ecol.* 2.
- Cowan, I. R. and F. L. Milthorpe. 1968. Plant factors in influencing the water status of plant tissues. In: *Water deficits and plant growth*. T. T. Kozlowski (ed.) Academic Press, N.Y.

- Ehlers, W., K. Baeumer, R. Stielpnagel, U. Köpke, and W. Böhm. 1981. Flow resistance in soil and plant during field growth of oats. *Geoderma* 25:1-12.
- Feddes, R. A. 1981. Water use models for assessing root zone modifications. In: *Modifying the root environment to reduce crop stress*. G. F. Arkin and H. M. Taylor (eds.) ASAE Monograph No. 4. Am. Soc. Agr. Eng. St. Joseph, Michigan.
- Gardner, W. R. 1964. Relation of root distribution to water uptake and availability. *Agron. J.* 56:41-45.
- Gardner, W. R. 1968. Availability and measurement of soil water. In: *Water deficits and plant growth*. T. T. Kozlowski (ed.). Academic Press, N.Y.
- Ginter-Whitehouse, D. L., T. M. Hinckley, and S. J. Pallardy. 1983. Spatial and temporal aspects of water relations of three tree species with different vascular anatomy. *For. Sci.* 29(2):317-329.
- Hanks, R. J. 1983. Yield and water use relationships: An overview. In: *Limitations to efficient water use in crop production*. H. M. Taylor, W. R. Jordan, and T. R. Sinclair (eds.). Am. Soc. Agron. Inc.
- Herkelrath, W. N., E. E. Miller, and W. R. Gardner. 1977. Water uptake by plants: II. The root contact model. *Soc. Sci. Am. J.* 41:1039-1043.
- Hsiao, T. C. and E. Acevedo. 1974. Plant responses to water deficits, water use efficiency and drought resistance. *Agric. Met.* 14:59-84.
- Hsiao, T. C. and K. J. Bradford. 1983. Physiological consequences of cellular water deficits. In: *Limitations to efficient water use in crop production*. H. M. Taylor, W. R. Jordan and T. R. Sinclair (eds.). Madison, Wisconsin.
- Jordan, W. R. and J. T. Ritchie. 1971. Influence of soil water stress on evaporation, root absorption, and internal water status of cotton. *Plant Physiol.* 48:783-788.
- Jung, Y.-S. and H. M. Taylor. 1984. Differences in water uptake rates of soybean roots associated with time and depth. *Soil Sci.* 137(5):341-349.
- Kiniry, L. N., C. L. Scrivner, and M. E. Keener. 1983. A soil productivity index based upon predicted water depletion and root growth. University of Missouri: Columbia Agricultural Experiment Station Bulletin 1051.
- Klepper, B. and H. M. Taylor. 1978. Limitations to current models describing water uptake by plant root systems. In: *The soil root interface*. Blackwells, Inc., Oxford.

- Klepper, B. 1983. Managing root systems for efficient water use: Axial resistances to flow in root systems - anatomical considerations. In: Limitations to efficient water use in crop production. H. M. Taylor, W. R. Jordan and T. R. Sinclair (eds.). Am. Soc. Agron. Inc. Madison, Wisconsin.
- Kozinka, V. 1981. Conducting efficiency of roots for the longitudinal flow of water. In: Structure and function of plant roots. R. Brouwer, O. Gasparikova, J. Kolek, and B. C. Loughman (eds.). Developments in Plant and Soil Sciences 4.
- Kozinka, V. 1981. Conducting efficiency of roots for the longitudinal flow of water. In: Structure and function of plant roots. R. Brouwer, O. Gasparikova, J. Kolek, and B. C. Loughman (eds.). Developments in Plant and Soil Sciences 4.
- Kozlowski, T. T. 1968. Introduction. In: Water deficits and plant growth. T. T. Kozlowski (ed.). Academic Press, N.Y.
- Meyer, W. S., E. L. Greacen, and A. M. Alston. 1978. Resistance to water flow in the seminal roots of wheat. *J. of Exp. Bot.* 29(113):1451-1461.
- Milburn, J. A. 1979. Water flow in plants. Longman Group Ltd., N.Y.
- Slatyer, R. O. 1967. Plant-water relationships. Academic Press, London.
- Stakgold, I. 1967. Boundary value problems of mathematical physics. Volume 1. Macmillan Co., N.Y.
- Sudar, R. A., K. E. Saxton, and R. G. Spomer, 1981. A predictive model of water stress in corn and soybeans. *Trans Am. Soc. Agric. Eng. Paper No. 79-2004.*
- Taylor, H. M. 1983. Managing root systems for efficient water use. In: Limitations to efficient water use in crop production. H. M. Taylor, W. R. Jordan and T. R. Sinclair (eds.). American Soc. Agron. Inc., Madison, Wisc.
- van Bavel, C. H. M. 1968. Hydraulic properties of a clay loam soil and the field measurement of water uptake by roots: I. Interpretation of water content and pressure profiles. *Soil Sci. Soc. Am. Proc.* 32:310-317.
- Wenkert, William. 1983. Water transport and balance within the plant: An overview. In: Limitations to Efficient Water Use in Crop Production. H. M. Taylor, W. R. Jordan, and T. R. Sinclair (eds.). Am. Soc. Agron. Inc.

Appendix A

List of Symbols

Symbol	Units	Description
$D_{h,k}$		a distribution parameter = $\int_0^1 \bar{u}_1(\sigma)\bar{h}_n(\sigma)d\sigma$
$h(y)$	T	the radial transfer coefficient
$\bar{h}(\sigma)$		transformed, dimensionless radial transfer coefficient
\bar{h}^*		special case, constant value of $\bar{h}(x)$
$\bar{h}_n(\sigma)$		the transfer coefficient distribution function
\bar{h}_T		$\int_0^1 h(\sigma)d\sigma$
H	LT	the overall radial-axial system conductance
\bar{H}		the transformed, dimensionless system conductance
k_x	L ² T	the axial conductivity
$\bar{k}_x(\sigma)$		the transformed, dimensionless axial conductivity
\bar{k}_x^*		special case constant value of $\bar{k}_x(\sigma)$
L	L	the total length of the axial pathway
q_x	L ³ T ⁻¹	the axial flux
\bar{q}_x		the transformed, dimensionless axial flow
\bar{u}_1		solution to the transformed, homogeneous flow equation which satisfies $\bar{u}'_1(0) = 0$ and $\bar{u}_1(1) = 1$
\bar{u}_2		solution to the transformed homogeneous flow equation which satisfies $\bar{u}_2(1) = 0$ and $\bar{u}'_2(1) = 1$
$\bar{w}(\sigma)$		the weighting function for the dimensionless soil water potential = $\bar{u}_1(\sigma) \cdot \bar{h}_n(\sigma)/D_{h,k}$
y	L	distance along the axial pathway
$\bar{\beta}^2(\sigma)$		the ratio $\bar{h}_T(\sigma)/\bar{k}_x(\sigma)$; the coefficient of the zero-order term in the governing flow equation for the special case, $\bar{k}_x(\sigma) = \bar{k}_x^*$
$\bar{\beta}^{*2}$		total radial to axial conductance ratio, $\bar{h}_T/\bar{k}_x(1)$, and coefficient of zero order term in the governing flow equation when $\bar{h}(\sigma) = \bar{h}^*$ and $\bar{k}_x(\sigma) = \bar{k}_x^*$; $\bar{\beta}^{*2} = h^*L^2/k^*$
σ		dimensionless distance along the axial pathway
$\Phi_1(\sigma)$		first integral term in the Green's function solution
$\Phi_2(\sigma)$		second integral term in the Green's function solution

Appendix A (continued)

Symbol	Units	Description
ψ	L^2T^{-2}	water potential
ψ_o	L^2T^{-2}	water potential at the outflow boundary $y = L$
$\psi_s(y)$	L^2T^{-2}	soil water potential
$\psi_x(y)$	L^2T^{-2}	axial water potential
$\tilde{\psi}$		transformed, dimensionless water potential
$\tilde{\psi}_s(\sigma)$		transformed, dimensionless soil water potential
$\tilde{\psi}_x(\sigma)$		transformed, dimensionless axial water potential
Ψ_s	L^2T^{-2}	the effective soil water potential
$\tilde{\Psi}_s$		the transformed, dimensionless effective soil water potential

Appendix B

The Back-Transformation Equations

The following equations provide the correspondence between variables in the original space-time frame and dimensionless variables defined on the unit interval $0 \leq \sigma \leq 1$. The equations are given here for convenience in interpreting the solutions to the dimensionless flow problem. Also, given below are corresponding constant terms in the dimensionless and original systems, and corresponding forms of key flow equations in the two systems.

Dimensionless Variable	Back-Transformation Equation
σ	$y = L \cdot \sigma$
$\tilde{\psi}$	$\psi = \psi_o \cdot (1 - \tilde{\psi})$
\tilde{q}_x	$q_x = q_o \cdot \tilde{q}_x$
\tilde{k}_x	$k_x = -q_o \cdot L \cdot \tilde{k}_x / \psi_o$
\tilde{h}	$h = -q_o \cdot \tilde{h} / \psi_o \cdot L$
\tilde{H}	$H = -q_o \cdot \tilde{H} / \psi_o$
$\tilde{\Psi}_s$	$\Psi_s = \psi_o \cdot (1 - \tilde{\Psi}_s)$
Constants	
$\sigma = 1$	$x = L$
$\tilde{\psi}_x = 0$	$\psi = \psi_o$
$\tilde{q}_x = 1$	$q_x = q_o$
$\beta^2 = \tilde{\beta}^{*2}$	$\beta^2 = L^2 \cdot \tilde{\beta}^{*2} = \beta^{*2}$
Equations	
$\tilde{q}_x(\sigma) = -\tilde{h}_x(\sigma) \cdot d\tilde{\psi}_x/d\sigma$	$q_x(y) = -k_x(y) \cdot d\psi_x/dy$
$d\tilde{q}_x/dx = \tilde{h}(\sigma) [\tilde{\psi}_s(\sigma) - \psi_x(\sigma)]$	$dq_x/dy = h(y) \cdot [\psi_s(y) - \psi_x(y)]$
$\tilde{H} \cdot \tilde{\Psi}_s = 1$	$H \cdot (\Psi_s - \psi_o) = q_o$

Appendix C

Listing of the BASIC Program used to Calculate $\tilde{\Psi}_{x'}$, $\tilde{q}_{x'}$, $D_{h,k}$
and Ψ_s for the Case of Constant \tilde{h} and \tilde{k}_x

```

1000 REM EFFECTIVE POTENTIAL
1005 D$ = CHR$(4)
1010 REM
1020 INPUT "H/K = ";B2
1030 BETA = SQR (B2)
1035 PRINT D$;"PR #1"
1040 PRINT "H/K = ";B2;"BETA = ";BETA
1050 PRINT " "
1060 PRINT " "
1070 C1 = EXP (BETA);C2 = EXP (- BETA)
1080 C3 = 0.5 * (C1 + C2)
1090 C4 = 0.5 * (C1 - C2)
1100 DHK = C4 / C3 / BETA
1110 EFPOT = (1.0 - C3) / C4 / BETA
1120 EFPOT = 1.0 + EFPOT
1125 FQ = (BETA * C4 + 1.) / C3
1126 FQ = 1. - FQ
1130 REM
1140 PRINT "DHK = ";DHK;"EFPOT = ";EFPOT
1150 PRINT " "
1160 PRINT " "
1165 SGMA = 0.0
1170 FOR I = 1 TO 10
1180 SGMA = SGMA + 0.1
1190 PR = BETA * SGMA
1200 E1 = EXP (PR)
1210 E2 = EXP (- PR)
1220 FCS = 0.5 * (E1 + E2)
1230 FSN = 0.5 * (E1 - E2)
1240 U1 = FCS / C3
1250 W = BETA * FCS / C4
1260 C5 = BETA * (1.0 - SGMA)
1270 C6 = EXP (C5)
1280 C7 = EXP (- C5)
1290 F3 = (C6 - C7) * 0.5
1300 AXPOT = (F3 / BETA - FCS) / C3
1310 AXPOT = AXPOT + SGMA
1320 F4 = 0.5 * (C6 + C7)
1330 AFLX = (BETA * FSN + F4) / C3
1340 AFLX = (1. - AFLX) / FQ
1345 PRINT "SIGMA =";SGMA
1350 PRINT "U1 =";U1
1360 PRINT "W =";W
1370 PRINT "AXIAL POTENTIAL = ";AXPOT
1380 PRINT "AXIAL FLUX =";AFLX
1385 PRINT " "; PRINT " "
1390 NEXT I
1395 PRINT D$;"PR #0"
1400 END

```

Appendix D

Program For Solving The Flow Problem With Constant Axial Conductivity

A FORTRAN program was written for the purpose of calculating the axial potential, $\tilde{\psi}_x(\sigma)$, the axial flux, $\tilde{q}_x(\sigma)$, the weighting function, $\tilde{w}(\sigma)$, the system distribution constant, $D_{h,k}$, the effective system conductance, \tilde{H} , the effective soil water potential, $\tilde{\Psi}_s$, and the flux reversal point, σ^* , for a linear, steady, radial-axial flow system. Names of principle program variables and their corresponding mathematical symbols are listed in Table D-1. The program was designed to solve the dimensionless flow problem, so transformation of output variables is necessary to arrive at the ordinary system counterparts. For example, the dimensionless position variable, X , ranges from 0 to 1 in the program output, and must be multiplied by the real length, L , of a corresponding axial flow pathway in order to arrive at the corresponding real position coordinate for that system. In the form shown here, the program is only capable of handling problems with constant axial conductivity. Therefore modification of the program would be required to treat problems with position-dependent axial conductivity. However, the program will handle a position dependent radial transfer coefficient in its present form.

Table D-1.
FORTTRAN names of major system variables.

Variable Name Text	FORTRAN Name
$\tilde{\psi}_x(\sigma)$	PHIX
$\tilde{\psi}_s(\sigma)$	PHI
$\tilde{w}(\sigma)$	W
$\tilde{u}_1(\sigma)$	u
$\tilde{q}_x(\sigma)$	Q
	X
$\tilde{k}_x(1) = \tilde{k}_x^*$	SCACON
\tilde{H}	SCAH
$\tilde{\Psi}_s$	PHIINT
$D_{h,k}$	HNUINT
\tilde{h}_T	SCAHB
β^{*2}	RESFAC
$\tilde{h}_n(\sigma)$	H
σ^*	ZER
$\tilde{\Psi}_x(\sigma^*) = \tilde{\Psi}_x^*$	PHI

The flow problem solved was derived from the two-point boundary value problem (12) – (12b). Equation (12) is first divided by \bar{k}_x^* , the constant axial conductivity. When the division by \bar{k}_x^* is carried out, the coefficient of $\tilde{\psi}_x(\sigma)$ in Equation 12 becomes

$$\bar{h}(\sigma)/\bar{k}_x^*.$$

Similarly, the coefficient of $\tilde{\psi}_s(\sigma)$ becomes

$$-\bar{h}(\sigma)/\bar{k}_x^*.$$

According to Equation 24 $\bar{h}(\sigma) = \bar{h}_n(\sigma) \bar{h}_T$ and by Equation 25, $\beta^{*2} = \bar{h}_T/\bar{k}_x(1) = \bar{h}_T/\bar{k}_x^*$. The above observations lead to the boundary value problem below, for the case $\bar{k}_x(\sigma) = \bar{k}_x^*$.

$$0 < \sigma < 1: d^2 \tilde{\psi}_x / d\sigma^2 - \beta^{*2} \bar{h}_n \tilde{\psi}_x = -\beta^{*2} \bar{h}_n \tilde{\psi}_s \quad (D-1)$$

$$\sigma = 0: d\tilde{\psi}_x / d\sigma = 0 \quad (D-1a)$$

$$\sigma = 1: \tilde{\psi}_x = 0 \quad (D-1b)$$

The above set of equations explicitly shows the nature of the problem solved by the program and indicates that values for β^{*2} , $\bar{h}_n(\sigma)$, and $\tilde{\psi}_s(\sigma)$ are the required input data for the program.

Program Strategy

It was previously shown with the Green's Function solution that if $\bar{k}_x(\sigma)$, $\bar{h}(\sigma)$, and $\tilde{\psi}_s(\sigma)$ are available, then all of the following functions can be obtained through various integral formulas: $\tilde{\psi}_x(\sigma)$, $\bar{q}_x(\sigma)$, $\bar{w}(\sigma)$, $D_{h,k}$, \bar{H} , and $\bar{\Psi}_s$. Closed form representations of these variables were generated from hyperbolic sine and cosine functions in the special case $\bar{h}(\sigma) = \bar{h}^*$ and $\bar{k}_x(\sigma) = \bar{k}^*$. However, to cope with situations where analytical expressions are not available for either $\bar{h}(\sigma)$ or $\bar{k}_x(\sigma)$, or when it is not possible to arrive at closed form solutions, a numerical approach was adopted. The procedure used in the program is described below, and the basic strategy for calculating the system functions from numerically computed $\tilde{\psi}_x(\sigma)$, $\tilde{\psi}_x'(\sigma)$, $\bar{u}_1(\sigma)$ and $\bar{u}_1'(\sigma)$ is as follows.

We first assume the availability of calculated $\tilde{\psi}_x(\sigma_k)$, $\bar{u}_1(\sigma_k)$, $\tilde{\psi}_x'(\sigma_k)$, and $\bar{u}_1'(\sigma_k)$ on a discrete grid-point set of σ_k which includes $\sigma_m = 1$. We further assume these computed values correspond to user supplied values of β^{*2} and $\bar{h}_n(\sigma_k)$, and $\tilde{\psi}_s(\sigma_k)$. If this is the case, then:

- (1) The dimensionless conductivity can be calculated from equation (32):

$$-\bar{k}_x(1) \tilde{\psi}_x'(1) = 1, \quad (32)$$

or since $\bar{k}_x(1) = \bar{k}_x^*$, we have $\bar{k}_x^* = -[\tilde{\psi}_x'(1)]^{-1}$.

- (2) The system distribution constant can be calculated from equation (40):

$$D_{h,k} = \bar{u}_1'(1)/\beta^{*2}.$$

- (3) Equation 25 can be used to calculate the total radial conductance from the value of \tilde{k}_x^* found in step (1) above. The total radial conductance can be obtained from

$$\tilde{h}_T = \beta^2 / \tilde{k}_x^*(1), \quad (25)$$

or

$$\tilde{h}_T = \beta^2 / \tilde{k}_x^*.$$

- (4) The weighting function $\tilde{w}(\sigma)$ can be computed from equation (36).

$$\tilde{w}(\sigma_k) = \tilde{h}_n(\sigma_k) \cdot \tilde{u}_1(\sigma_k) / D_{h,k} \quad (36)$$

- (5) The effective system conductance is (Eq. 38):

$$\tilde{H} = \tilde{h}_T \cdot D_{h,k} \quad (38)$$

- (6) Finally, the effective soil water potential can be calculated from equation (35).

$$\tilde{H} \Psi_s = 1. \quad (35)$$

so

$$\Psi_s = \tilde{H}^{-1}.$$

In addition to the above quantities the program provides estimates of the axial flux-reversal point σ^* and the corresponding maximum axial potential, $\tilde{\psi}_x^*$ lead to values for the various calculated quantities that are identical to corresponding quantities of the sequence.

Description of Numerical Procedures

The program performs four basic tasks; each of these tasks requires a specific scheme:

- (1) Solution of the flow problem (6) – (6b) for the axial potential $\tilde{\psi}_x(\sigma)$, and its derivative $\tilde{\psi}_x'(\sigma)$, on a discrete set of σ_k in the interval $0 \leq \sigma \leq 1$.
- (2) Solution of the auxiliary flow problem for $\tilde{u}_1(\sigma)$ and its derivative, $\tilde{u}_1'(\sigma)$.
- (3) Calculation of the system functions \tilde{H} , $\tilde{\psi}_x$, $D_{h,k}$, and the weighting function, $\tilde{w}(\sigma_k)$ (as per the outline of the preceding section).
- (4) Calculation of the flux reversal point σ^* and the corresponding maximum axial potential, $\tilde{\psi}_x^*$.

The program employs a shooting procedure (Carnahan et al.) for solving the two boundary value problems (Task 1 and Task 2). The steps 1-6 outlined above were incorporated into the program for obtaining the system functions (Task 3). Finally, an interpolation procedure (Task 4) was included to obtain the flux-reversal point and maximum axial potential from the set of values, $\tilde{\psi}_x(\sigma_k)$ and $\tilde{\psi}_x'(\sigma_k)$, generated in the numerical solution to the main flow problem.

Numerical Solution of the Boundary Value Problems

The radial-axial flow system was described as a boundary value problem (6) – (6b) in the position-dependent axial potential, $\tilde{\psi}_x(\sigma)$. The Green's function solution to this problem utilizes linearly independent solutions, $\tilde{u}_1(\sigma)$ and $\tilde{u}_2(\sigma)$, to the system's associated homogeneous equation (6c). In the approach taken here, the function $\tilde{u}_1(\sigma)$ was uniquely determined by specifying its value, $\tilde{u}_1(1) = 1$, at $\sigma = 1$. This condition along with the already specified value $\tilde{u}_1(0) = 0$ led to an auxiliary flow problem in which $\tilde{u}_1(\sigma)$ can be interpreted as a hypothetical water potential function. The two boundary value problems, one in $\tilde{\psi}_x$ and one in \tilde{u}_1 , lend themselves to solution by a shooting technique (Carnehan et al., 1969) in which the original boundary value problem is temporarily replaced with an initial value problem. The substituting initial value problem is then solved by a Fourth Order Runge-Kutta procedure and the resulting solution to this initial value problem is used to make an improved approximation to the boundary value problem. This sequence of approximation and solution is repeated until a pre-set convergence criterion is met, and the computed solution of the most recent initial value approximation is accepted as the solution to the boundary value problem. Some of the details of the shooting procedure are given here. For more details the reader is referred to Carnahan et al. (1969).

For either the $\tilde{\psi}_x$ or \tilde{u}_1 problem the approximating initial value problem is obtained from the original boundary value problem in two steps:

- (a) Sacrificing the right end point boundary condition at $\sigma = 1$.
 - (b) Providing a second (artificial) condition at the left end point $\sigma = 0$.
- For the $\tilde{\psi}_x$ problem the condition at $\sigma = 1$ (Eq. D-16) is $\tilde{\psi}_x(1) = 0$. To obtain the first approximating initial value problem, this condition is replaced with: $\tilde{\psi}_x(0) = 0.25$. The approximating problem is therefore comprised of equation (D-1) together with the two initial conditions $\tilde{\psi}'_x(0) = 0$ and $\tilde{\psi}_x(0) = 0.25$. For the \tilde{u}_1 problem, $\tilde{u}_1(1)$ is replaced by $\tilde{u}_1(0) = 0.25$, to arrive at the approximating initial value problem.

Revised Approximations

Following the solution of the approximating initial value problem in $\tilde{\psi}_x$, the calculated value of $\tilde{\psi}_x(1)$ is compared with the desired value $\tilde{\psi}_x(1) = 0$. If there is agreement between these two values to within a specified tolerance, the solution to the initial value problem is accepted as the solution to the boundary value problem. If the calculated $\tilde{\psi}_x(1)$ is too large, a new approximating initial value is provided according to the formula:

$$b_{j+1} = b_j - [\tilde{\psi}_x(1)]_j / c_j \quad (D-2)$$

where b_j is the most recently used estimate of $\tilde{\psi}_x(0)$ and $[\tilde{\psi}_x(1)]_j$ is the most recently calculated value of $\tilde{\psi}_x(1)$. The number c_j is an estimate of the rate of change in $\tilde{\psi}_x(1)$ with respect to a change in $\tilde{\psi}_x(0)$:

$$c_j = [\tilde{\psi}_x(1)_j - \tilde{\psi}_x(1)_{j-1}] / b_j \quad (D-3)$$

The above formula fails on the first and second passes, when $j = 1$ and $j = 2$, since there is no preceding estimate, b_{j-1} , for either case. On the first pass, b_1 , is given the initial guess value 0.25. At the end of the first pass, the numerator of c_j (equation D-3) is obtained as the difference between the calculated value of $\tilde{\psi}_x(1)$ and 0, and the denominator is assigned the value, 1. The net affect of calculations in the program results in a second starting estimate of 0.125. At the end of the second pass, the above formula for b_{j+1} takes effect, and the convergence is accelerated. As was previously indicated, when the calculated value of $\tilde{\psi}_x(1)$ is acceptably close to 0, iteration is terminated.

In the case of the \tilde{u}_1 problem it is not necessary to go through an iterative revision of the approximating initial value problem. The reason for this stems from three characteristics of the \tilde{u}_1 problem, in addition to its basic linearity. The governing equation (6c) for the \tilde{u}_1 problem is homogeneous, the left-end boundary condition is homogeneous, and the right end boundary condition is non-zero: $\tilde{u}_1(1) = 1$. Since this is the case, all of the values of $\tilde{u}_1(\sigma_k)$ which are calculated in the solution to the first approximating initial value problem, are simply divided by the calculated value of $\tilde{u}_1(1)$. The resulting, revised set of $\tilde{u}_1(\sigma_k)$ comprises a numerical solution which satisfies both the governing equation (6c) and the two boundary conditions $\tilde{u}_1(0) = 0$ and $\tilde{u}_1(1) = 1$.

Fourth Order Runge-Kutta Procedure

Each of the approximating initial value problems is solved by a standard quadrature procedure which is discussed in detail by Carnahan et al. (1969). The specific format used in this program requires that each of the governing second order differential equations be rewritten as a pair of first order equations. Thus equation (D-1) for the $\tilde{\psi}_x$ problem is expressed as the pair:

$$dV_1/d\sigma = f_1(\sigma) \quad (D-4)$$

$$dV_2/d\sigma = f_2(\sigma), \quad (D-5)$$

where $V_1 = \tilde{\psi}_x$, $V_2 = \tilde{\psi}'_x$, $f_1(\sigma) = V_1$ and $f_2(\sigma) = \beta^{*2} \tilde{h}_n(\sigma) [V_1(\sigma) - \tilde{\psi}_s(\sigma)]$. It can be verified that if appropriate substitutions are made, the above system of equations reduces to (D-1). In the above notation, the original boundary condition (D-1a) becomes $V_2(\sigma) = 0$, and the temporary initial condition, supplied in the shooting procedure: $\tilde{\psi}_x(0) = 0.25$, becomes $V_1(0) = 0.25$.

The auxillary flow problem in u_1 is likewise rewritten in a form identical to the pair of equations (D-4) and (D-5). The difference is that for the \tilde{u}_1 problem, $V_1(\sigma) = \tilde{u}_1$, $V_2(\sigma) = \tilde{u}'_1$, $f_1(\sigma) = V_1$ and $f_2(\sigma) = \beta^{*2} \tilde{h}_n(\sigma) V_1(\sigma)$. The chief distinguishing feature is the explicit form of the function $f_2(\sigma)$, which contains the additional term $\beta^{*2} \tilde{h}_n(\sigma) \tilde{\psi}_s(\sigma)$ in the $\tilde{\psi}_x$ problem, but not in the \tilde{u}_1 problem.

Structure of the numerical solution

The numerical solution to any of the approximating initial value problems is obtained as a discrete set of values, either $\tilde{\psi}_x(\sigma_k)$ or $\tilde{u}_1(\sigma_k)$, on a grid $\sigma_1 = 0, \sigma_2, \dots, \sigma_{n-1}, \sigma_n = 1$. In the notation used in equation (D-4) and (D-5) the solution values are $V_1(\sigma_1), V_1(\sigma_2), \dots, V_1(\sigma_n), V_2(\sigma_1), V_2(\sigma_2), \dots, V_2(\sigma_n)$. The V_1 's correspond to the values of $\tilde{\psi}_x(\sigma_k)$ and V_2 's to $\tilde{\psi}'_x(\sigma_k)$. Similarly, for the \tilde{u}_1 problem the V_1 's correspond to $\tilde{u}_1(\sigma_k)$ and the V_2 's to $\tilde{u}'_1(\sigma_k)$. The integration procedure utilizes the Runge-Kutta algorithm in a step-wise manner. The values of $V_1(0)$ and $V_2(0)$ are available at the outset as boundary data. The algorithm then leads to calculated values of $V_1(\sigma_2)$ and $V_2(\sigma_2)$. The same algorithm is then used to calculate $V_1(\sigma_3)$ and $V_2(\sigma_3)$, and so on until all of the V_1 's and V_2 's are computed on the σ_k grid. The grid step-size $\Delta\sigma_k = \sigma_{k+1} - \sigma_k$ is variable and adjusted for each successive step.

The Solution Algorithm

The program contains a FUNCTION SUBPROGRAM RUNGE, which is similar to the one discussed by Carnahan et al. (1969). This subprogram embodies a fourth-order Runge-Kutta algorithm, with Kutta coefficients, for advancing the solution to an initial value problem across the interval $0 \leq \sigma \leq 1$. The structure of the subprogram and the interdependence of the Kutta coefficients, both internally, and through quantities calculated in the

main program, requires that five calls be made to RUNGE for each grid step. Aside from the listing of the program, which can be found in the appendix, the reader is referred to the above reference for further details of the Runge-Kutta program used to solve the flow problem.

Interpolation for the Axial Flux-Reversal Point and Maximum Axial Potential

For some combinations of β^*2 , \tilde{h}_n , and $\tilde{\psi}_s$, the dimensionless axial flux will take on negative values over some subinterval of $0 \leq \sigma \leq 1$. The only way this can happen is if there is a predicted transmittal of water from the interior of the axial flow region to the surrounding soil region. Such reverse flows, or leakage, can occur even if the outflow boundary potential, ψ_0 , is lower than the minimum value of soil water potential, ψ_s , in the supply region. A procedure was incorporated in the program for isolating the position, σ^* , of an axial flow reversal. The procedure also leads to the corresponding dimensionless axial potential $\tilde{\psi}_x^*$ value. The three main steps in the procedure are:

- (1) Isolation of the σ - subinterval (σ_i, σ_{i+1}) over which the reversal occurs. This step is carried out by individually examining the calculated $\tilde{\psi}'_x$ values and by flagging the two: σ_k, σ_{k+1} values between which the sign of $\tilde{\psi}'_x$ changes.
- (2) Once the two σ values are flagged, a cubic interpolation procedure is used to calculate the value of σ^* .
- (3) The cubic interpolation polynomial generated in step 2 is used to calculate the value of σ^* , such that $\tilde{\psi}'_x(\sigma^*) = 0$. The procedure utilizes the values of $\sigma_k, \sigma_{k+1}, \tilde{\psi}_x(\sigma_k), \tilde{\psi}'_x(\sigma_k), \tilde{\psi}_x(\sigma_{k+1})$ and $\tilde{\psi}'_x(\sigma_{k+1})$.
- (4) The cubic interpolation polynomial generated in step 2 is used to calculate the value of $\tilde{\psi}_x(\sigma^*) = \tilde{\psi}_x^*$.

The cubic interpolation scheme is as follows.

The cubic polynomial is of the form:

$$\tilde{\psi}_x(\sigma) = A + B \sigma + C \sigma^2 + D \sigma^3.$$

The following constraints are imposed:

$$(a) \tilde{\psi}'_x(\sigma^*) = 0 \text{ or } B + 2C\sigma^* + 3D\sigma^{*2} = 0$$

$$(b) \tilde{\psi}_x(\sigma_k) = A + B\sigma_k + C\sigma_k^2 + D\sigma_k^3$$

$$(c) \tilde{\psi}'_x(\sigma_k) = B + 2C\sigma_k + 3D\sigma_k^2$$

$$(d) \tilde{\psi}_x(\sigma_{k+1}) = A + B\sigma_{k+1} + C\sigma_{k+1}^2 + D\sigma_{k+1}^3$$

$$(e) \tilde{\psi}'_x(\sigma_{k+1}) = B + 2C\sigma_{k+1} + 3D\sigma_{k+1}^2$$

Once the values of σ_k and σ_{k+1} have been flagged, the terms on the left hand sides of equations (b) – (d) are known quantities, along with σ_k and σ_{k+1} . The system of four equations in the unknowns A, B, C, and D were solved by a row-reduction and back substitution scheme so that A, B, C, and D can be calculated explicitly in terms of the known quantities. The quadratic formula is applied to equation (a) to calculate σ^* from the supplied values of B, C, and D. The last step is calculation of $\tilde{\psi}_x^*$ from σ^* , using the cubic polynomial, equation (d).

Program Variables and Flow During Execution

The major segments of code in the main program are: (1) Initialization, lines 7-14; (2) Numerical solution procedure, including the Runge-Kutta procedure, lines 15-79; (3) Calculation of system variables, lines 80-99; (4) Calculation of zero flux point and maximum axial potential, lines 100-102; (5) Optional check procedure, line 103 and (6) Output to printer line 104. Related segments of code occur in various subprograms.

RUNGE, lines 112-142, contains the Runge-Kutta procedure; PHIS, lines 107-110, calculates the dimensionless soil water potential; STAR, lines 143-198, calculates the flux reversal point; CHECK, lines 198-226, compares the numerical and analytical solutions for constant h and k; HNORM, lines 227-295, calculates the value of the transfer coefficient distribution; OUTPUT, lines 296-367, print results.

1. Initialization

Some of the program variables are assigned initial values in lines 7-24. FORTRAN names of major program variables, together with a brief description of each, is shown in Table D-2.

2. Numerical Solution Procedure

The part of the code devoted to the solution of the two boundary value problems occupies lines 15-79 in the main program, and lines 112-142 in FUNCTION RUNGE. U(1) and U(2) are assigned values corresponding to $X = 0$ and $KPT = 1$ in lines 18 and 19. The dimensionless soil water potential PHI is evaluated by the call to PHIS(X) in line 22 and the normalized transfer coefficient distribution H is evaluated by the call to HNORM(X. . .) in line 23. Following initialization of these variables, control goes to line 36 (#20), and the values of X, PHI, H, U(1), and U(2) are stored

for $KPT = 1$. KPT is incremented in line 51 and control passes back to line 26 (#10) where the first call to RUNGE is made. The only calculations made on the first call are of a set-up nature. The variable RUNGE is assigned the value 1 and this value is returned to the main program as KM.

Table D-2.
Description of major program variables.

KPT	current value of grid point index
X	current value of dimensionless position; corresponds to σ_k , and is initialized to 0.0
PHI	value of dimensionless soil water potential at current value of X; corresponds to $\tilde{\psi}_s(\sigma_k)$
DX	variable step size in FUNCTION RUNGE; corresponds to $\sigma_{k+1} - \sigma_k$
H	value of transfer coefficient distribution at current value of X; corresponds to $\tilde{h}_n(\sigma_k)$
PHIX	value of dimensionless axial potential distribution at current value of X; corresponds to $\tilde{\psi}_x(\sigma_k)$
W	value of weighting function at current value of X; corresponds to $\tilde{w}(\sigma_k)$
Q	Dimensionless axial flux; corresponds to $\tilde{q}_x(\sigma_k)$
U(1)	function value (either axial potential or auxiliary potential) at current value of X; corresponds to $\tilde{\psi}_x(\sigma_k)$ if $HOM = 1$ or to $\tilde{u}_1(\sigma_k)$ if $HOM = 0$
U(2)	value of calculated derivative returned from RUNGE at current value of X; corresponds to $\tilde{\psi}'(\sigma_k)$ if $HOM = 1$ or to $\tilde{u}'(\sigma_k)$ if $HOM = 0$
RESFAC	supplied value of the radial-to-axial conductance ratio, β^*2
SCACON	calculated dimensionless axial conductivity, $\tilde{k}_x(1) = \tilde{k}_x^*$
SCAH	calculated dimensionless effective radial-axial conductance
SCAHB	calculated dimensionless total radial conductance
HNUINT	calculated system distribution constant, $D_{h,k}$
PHIINT	calculated effective soil water potential

Table D-2 (continued).

ZER	calculated value of the zero-flux point
PHI	calculated value of the maximum axial potential
M	total number of grid points used in solution to \bar{u}_1 problem
N	total number of grid points used in solution to $\tilde{\psi}_x$ problem
NFUN	indicator variable used to designate one among several transfer coefficient distributions supplied in FUNCTION HNORM
ERROR	user-supplied value of the tolerance for acceptance of the approximating initial value problem in the shooting procedure

FUNCTION HNORM is called to evaluate the transfer coefficient distribution and the nonhomogeneous terms F(1) and F(2) in the two first order equations for the $\tilde{\psi}_x$ problem (Eq. D-4 and Eq. D-5), are calculated in lines 30 and 31. The variable BETA2 (line 29) is the product of the normalized transfer coefficient distribution, H, and the total radial to axial conductance ratio, RESFAC. Regardless of whether the $\tilde{\psi}_x$ (HOM = 1) or \bar{u}_1 (HOM = 0) problem is being solved, line 30 is used to calculate F(1):

$$F(1) = U(2)$$

If HOM = 0 (\bar{u}_1 problem) F(2) is calculated as:

$$F(2) = \text{BETA2} * U(1)$$

If HOM = 1 ($\tilde{\psi}_x$ problem) F(2) is calculated as:

$$F(2) = \text{BETA2} * U(1) - \text{BETA2} * \text{PHI}$$

(See lines 31 and 34 of the program.)

The difference in the two above formulas for F(2) corresponds directly to the previously indicated difference in the systems of first order equations (D-4) and (D-5) for the two boundary value problems being solved. (See discussion related to D-4 and D-5).

Following the calculation of F(2), control is transferred to statement 10 (line #26) where a second call is made to FUNCTION RUNGE. Five calls to RUNGE are needed before all of the calculations of the function and its derivative are complete. The final calculations of U(1) and U(2) for each subinterval are made on the fifth call. On the return from the fifth call, the value of RUNGE is returned as 0, and control transfers to statement 20 (line 36). All values that were generated during calculations for that subinterval, and that are to be saved, are then stored in designated arrays. If HOM = 0, the position variable X, is passed to XS(KPT), U(1) to U1(KPT), and H to

HN(KPT). If $HOM = 1$, X is stored as $XS1(KPT)$, the soil water potential, PHI , as $PHIST(KPT)$, the derivative value $U(2)$ as $Q(KPT)$ and the function value corresponding to the axial potential $U(2)$ is stored as $PHIX(KPT)$.

Following the calculations and storage of values for each subinterval, a check is made (line 50) to see if the current value of X is 1.0. If not, KPT is incremented by 1. If X is 0.0, control goes to statement 10 and calculations are revised for the first subinterval, with the step size $DX = 0.1$. If X is greater than 0, the step size DX is adjusted if necessary, so that the quantity $F(2)*DX$ is no larger than 0.1 (line 56). A check is then made to insure that $X + DX$, for the next step, does not exceed 1. If it does exceed 1, DX is calculated so that $X + DX$ exactly equals 1. Calculations are then initiated for the next subinterval.

When $U(1)$ and $U(2)$ have been obtained for the final subinterval and $X = 1.0$, control transfers from line 50 to statement 35 in line 60. A check is made to determine which problem is in progress. If $HOM = 0$, indicating the \tilde{u}_1 problem, a transfer is made to statement 44 (line 88) where HOM is reassigned the value 1.0 and the current value of KPT is saved as N , the total number of grid points for the u_1 problem. Control is passed back to line 9, statement 1, and calculations proceed for the $\tilde{\psi}_x$ problem.

If the check at line 61 reveals $HOM = 1$, the procedure for calculating a revised estimate of the initial value, $U10$, for the $\tilde{\psi}_x$ problem is initiated. If the current value of $U(1)$, which at this point contains the value of $\tilde{\psi}_x(1)$, is sufficiently close to 0.0, there is no need for further iteration on the $\tilde{\psi}_x$ problem. When convergence is achieved, control passes to statement 40 (line 79). Otherwise, an estimate of a new initial value is made (lines 65-77) and solution of the new initial value problem approximation to the $\tilde{\psi}_x$ problem is resumed in line 15 (statement 5).

Once convergence is determined by the comparison of $U(1)$ with 0.0 in line 64, calculation of the system variables is initiated in line 80.

Calculation of System Variables

It was previously pointed out that the values $\tilde{u}'_1(1)$ and $\tilde{\psi}'_x(1)$ play a key role in the computation of the system functions. Following the solution of the $\tilde{\psi}_x$ problem, the value of $U(2)$ is the correct, required value of $\tilde{\psi}_x(1)$. However, the stored value of $U(2)$, following solution of the \tilde{u}_1 problem, does not correspond to the required $\tilde{u}'(1)$. The reason for this is that only the solution to the approximating initial value problem, with $\tilde{u}_1(0) = 0.25$ and $u'(0) = 0$ is obtained with the Runge-Kutta solution. Upon completion of this solution, the calculated $U(1)$ and $U(2)$, which correspond to unadjusted values of the function and its derivative, are saved as $U11S$ and $U1P$, respectively (lines 41 and 47). Following completion of the $\tilde{\psi}_x$ problem calculations, $U11S$ is used to obtain the required value of the derivative ($\tilde{u}'_1(1)$) in line 80:

$$U1P = U1P/U11S.$$

The variable SCACON corresponds to the dimensionless axial conductivity \bar{k}_x^* . The dimensionless system conductance is calculated as SCACON*U1P (line 83). The dimensionless soil water potential PHIINT is calculated in line 84, and the distribution constant $D_{h,k}$ is calculated HNUINT = U1P as RESFAC) (line 86).

Following computation of HNUINT, control is transferred to statement 45 (line 91). The number of grid points for the $\bar{\psi}_x$ problem is stored as M, the function values ($\bar{u}_1(\sigma_i)$) for the \bar{u}_1 problem are adjusted in line 94 and the weighting function ($\bar{w}(\sigma)$) is calculated as W(I) in line 95. Calculation of the flux reversal point, maximum axial potential, and the optional check procedure occurs in lines 100-103. The results of the run are printed through FUNCTION OUTPUT.

C JOB

C

C

C

C

C

C

C

C

C

C

C

C

C

C

C

C

C

C

C

C

C

C

C

C

C

C

C

C

C

C

C

C

C

C

C

C

C

C

C

THIS PROGRAM GENERATES THE EFFECTIVE SOIL-ROOT CONDUCTANCE,, EFFECTIVE SOIL WATER POTENTIAL, AND AXIAL POTENTIAL-, AXIAL FLUX-, AND NORMALIZED WEIGHTING FUNCTION- DISTRIBUTIONS FOR A CONTINUOUS RADIAL-AXIAL FLOW SYSTEM.

PRESENT APPLICATION: THE FLOW IS ASSUMED TO OCCUR IN RESPONSE TO POTENTIAL GRADIENTS SET UP AS A RESULT OF:

A. SOIL WATER POTENTIAL(PHI) DISTRIBUTION ALONG, BUT EXTERNAL TO, THE ROOT SYSTEM AXIAL PATHWAY.

B. AXIAL POTENTIAL AT THE TERMINAL END OF THE PATHWAY.

C. TRANSFER COEFFICIENT (HN(X)) DISTRIBUTION ALONG THE PATHWAY-- THE AXIAL FLUX IS ASSUMED TO BE AUGMENTED ACCORDING TO

$DQ/DX = HN*(PHI-PHIX)$, WHERE

Q = DIMENSIONLESS AXIAL FLUX AND PHIX = DIMENSIONLESS AXIAL POTENTIAL.

D. THE AXIAL CONDUCTIVITY (KX) DEFINED BY THE EQUATION

$Q = -KX*D(PHIX)/DX$.

KX IS ASSUMED TO BE CONSTANT. A MINOR ALTERATION OF THE PROGRAM IS REQUIRED TO ACCOMODATE VARIABLE KX. KX DOES NOT APPEAR IN THE PROGRAM EXPLICITLY. IT'S INFLUENCE IS INCLUDED IN THE RADIAL-TO-AXIAL TOTAL CONDUCTANCE RATIO, RESFAC.

SOLUTION PROCEDURE: ALL CALCULATED VALUES ARE BASED ON NUMERICAL SOLUTIONS TO THE TWO LINEAR FLOW PROBLEMS:

(1) $D(DY/DX)/DX - B*HN(X)*Y = PHI$

$Y'(0) = 0$

$Y(1) = 0$

AND

(2) $D(DY/DX)/DX - B*HN(X)*Y = 0$

$Y'(0) = 0$

$Y(1) = 1.$

C IN PROBLEM (1) Y CORRESPONDS TO AXIAL POTENTIAL (PHIX). IN PROBLEM(2)
 C Y CORRESPONDS TO THE FUNCTION (U1) WHICH IS USED TO GENERATE THE
 C NORMALIZED WEIGHTING FUNCTION (W).
 C

C IN BOTH PROBLEMS B (RESFAC BELOW) IS THE RADIAL-TO AXIAL TOTAL CON-
 C DUCTANCE RATIO.
 C

C X IS DIMENSIONLESS DISTANCE ALONG THE AXIAL FLOW PATHWAY: $X = Z/L$,
 C WHERE Z IS REAL DISTANCE AND L = PATH LENGTH.
 C

C THE FOLLOWING QUANTITIES APPEAR IN THE OUTPUT FROM THIS PROGRAM:

C X DIMENSIONLESS DISTANCE

C U SOLUTION TO PROBLEM (2) ABOVE

C W NORMALIZED WEIGHTING FUNCTION

C PHIX DIMENSIONLESS AXIAL POTENTIAL

C Q DIMENSIONLESS AXIAL FLUX

C SCACON DIMENSIONLESS AXIAL CONDUCTIVITY

C SCAH DIMENSIONLESS EFFECTIVE SOIL-ROOT SYSTEM CONDUCTANCE

C HN DIMENSIONLESS TRANSFER COEFFICIENT DISTRIBUTION

C PHI DIMENSIONLESS SOIL WATER POTENTIAL

C RESFAC RADIAL-TO-AXIAL TOTAL CONDUCTANCE RATIO

C ZER ZERO-FLUX POINT

C PHI MAXIMUM POTENTIAL (AT ZERO-FLUX POINT)

C RESFAC, PHI, AND HN MUST BE SUPPLIED AS INPUT. THE REMAINING VAR-
 C IABLES ARE CALCULATED. PHI IS INPUT TO THE MAIN PROGRAM THROUGH
 C FUNCTION PHIS. HN IS SUPPLIED THROUGH FUNCTION HNORM.

C RESFAC, A TRANSFER COEFFICIENT DISTRIBUTION IDENTIFIER (NFUN), AND
 C AN ERROR TOLERANCE FOR THE CONVERGENCE OF THE SOLUTION TO PROBLEM (1)
 C (ERROR) ARE CURRENTLY THE ONLY INPUT WHICH MUST BE SUPPLIED THROUGH
 C A DATA INITIALIZATION OR READ STATEMENT IN ORDER FOR THE PROGRAM TO
 C EXECUTE.(SEE CURRENT LISTING OF FUNCTION HNORM FOR PROPER USE OF
 C NFUN.)

C THE DIMENSIONLESS VARIABLES ARE RELATED TO VARIABLES IN ANY CORRESPON-
 C DENT DIMENSIONAL SYSTEM AS FOLLOWS:

C DIMENSIONAL SYSTEM: $L = \text{PATHLENGTH}$, $FO = \text{FLUX AT } Z = L$, $PSIO = \text{AXIAL}$
 C $\text{POTENTIAL AT } Z = L$.

C TO OBTAIN THE LISTED VARIABLE IN THE CORRESPONDENT DIMENSIONAL
 C SYSTEM:

C POTENTIAL MULTIPLY DIMENSIONLESS POTENTIAL BY $-PSIO$
 C AND ADD $PSIO$.

```

C          FLUX          MULTIPLY Q BY F0
C
C          EFFECTIVE POTENTIAL
C          EFFECTIVE SYSTEM CONDUCTANCE          MULTIPLY SCAH BY -F0/PSI0.
C          DISTANCE          MULTIPLY X BY L.
C
C          A FOURTH-ORDER RUNGE-KUTTA TECHNIQUE FOR SOLVING A DERIVED
C          FIRST-ORDER INITIAL VALUE PROBLEM IS EMPLOYED FOR THE SOLUTION
C          OF BOTH PROBLEMS (1) AND (2). ONLY ONE PASS IS REQUIRED TO SOLVE
C          PROBLEM (2). IN THIS CASE THE BOUNDARY CONDITION AT X = 1 IS MET
C          BY DIVIDING THE SOLUTION VALUE AT EACH POINT BY THE CALCULATED VALUE
C          AT X = 1. PROBLEM (2) IS SOLVED BY ITERATING WITH THE INITIAL-VALUE
C          SOLUTION AND ADJUSTING THE ESTIMATED INITIAL CONDITION UNTIL
C          THE CONDITION AT X = 1 IS MET.
C
C-----
C-----
C
1  DIMENSION F(2),U(2),U1(100),W(100),PHIX(100),DPHIX(100),XS(100)
2  DIMENSION HN(100),Q(100),PHIST(100),PHICLK(100)
3  DIMENSION DIFCHK(100),XS1(100)
4  COMMON N,M,NFUN,SCACON,SCAH,PHIINT,RESFAC,ZER,PHI,HNUINT,SIGH
5  COMMON PHIX,PHIST,Q,HN,W,XS,XS1,U1,ERROR
6  INTEGER RUNGE
C
C          SUPPLY VALUES OF NFUN, RESFAC, AND ERROR FOR THIS RUN.
C
7  DATA RESFAC/0.1/, NFUN/1/, ERROR/0.0002/
C
C          INITIALIZE FOR OUTER LOOP: SOLUTION OF PROBLEMS (1) AND (2) ABOVE.
C          ON THE FIRST PASS (HOM = 0.0) PROBLEM (2) IS SOLVED FOR THE FUNCTIONS
C          U AND W. THE SECOND PASS (HOM = 1.0) CONSTITUTES THE FIRST ITERATION
C          FOR SOLVING PROBLEM (1) FOR PHIX AND Q.
C
8  HOM = 0.0
9  1 ICOUNT = 0
10 U1L = 0.0
11 U1R = 0.5
12 DU0 = 1.0
13 U(1) = 0.0
14 U10 = 0.25
C
C          INITIALIZE FOR RUNGE-KUTTA SOLUTION OF INITIAL-VALUE PROBLEM.
C
15 5 CONTINUE
16 UOOLD = U10
17 UIOLD = U(1)
18 U(1) = U10
19 U(2) = 0.0
20 X = 0.0
21 DX = 0.1
22 PHI = PHIS(X)
23 H = HNORM(X,NFUN,HMOM,SIGH)
24 KPT = 1
25 GO TO 20
C
C          BEGIN RUNGE-KUTTA SOLUTION TO ESTIMATE VALUES OF U(1) AND U(2) AT
C          X + DX GIVEN THEIR VALUES AT X. FIVE PASSES MUST BE MADE THROUGH
C          FUNCTION RUNGE AND F(1) AND F(2) MUST BE EVALUATED FOUR TIMES
C          TO COMPLETE THE STEP OF LENGTH DX.
C
26 10 KM = RUNGE(2,U,F,X,DX)
27 IF(KM.NE.1) GO TO 20

```

```

C
C      EVALUATE THE DIMENSIONLESS TRANSFER COEFFICIENT DISTRIBUTION AT
C      THE CURRENT VALUE OF X.
C
28      H = HNORM(X,NFUN,HMOM,SIGH)
29      BETA2 = RESFAC*H
30      F(1) = U(2)
31      F(2) = BETA2*U(1)
32      IF(HOM.EQ.0.0) GO TO 10

C
C      EVALUATE THE DIMENSIONLESS SOIL WATER POTENTIAL AT THE CURRENT
C      VALUE OF X.
C
33      PHI = PHIS(X)
34      F(2) = F(2)-BETA2*PHI
35      GO TO 10
36      20 CONTINUE
37      IF(HOM.EQ.0.0) GO TO 25

C
C      STORE POSITION (X) AND R-K SOLUTION VALUES FOR CURRENT GRID-POINT.
C
38      XSI(KPT) = X
39      PHIS(KPT) = PHI
40      Q(KPT) = -U(2)
41      PHIX(KPT) = U(1)
42      GO TO 30

C
C      STORE POSITION (X) AND R-K SOLUTION VALUES FOR CURRENT GRID-POINT.
C
43      25 U1(KPT) = U(1)
44      XS(KPT) = X
45      HN(KPT) = H
46      U1S = U(1)
47      U1P = U(2)
48      W(KPT) = H*U(1)
49      30 CONTINUE

C
C      IF X IS LESS THAN 1, CONTINUE RUNGE-KUTTA INTEGRATION.
C
50      IF(X.GE.1.0) GO TO 35
51      KPT = KPT+1
52      IF(X.EQ.0.0) GO TO 10
53      DX = 0.1
54      F2 = F(2)
55      FABS = ABS(F2)

C
C      ADJUST THE VALUE OF DX IF NECESSARY.
C
56      IF(FABS.GT.1.0) DX = 0.1/FABS
57      DIFONE = 1.0-X
58      IF(DX.GT.DIFONE) DX = 1.0-X
59      GO TO 10
60      35 CONTINUE
61      IF(HOM.EQ.0.0) GO TO 44
62      UDIF = U(1)
63      ABSDIF = ABS(UDIF)

C
C      CHECK FOR CONVERGENCE IN BOUNDARY CONDITION AT X = 1. IF
C      CONVERGENCE HAS NOT OCCURRED, ESTIMATE NEW INITIAL VALUE (I.E. PHIX AT
C      X = 0) AND BEGIN NEXT ITERATION STEP.
C
64      IF(ABSDIF.LE.ERROR) GO TO 40
65      U1NEW = U(1)
66      DU1 = U1NEW-U1OLD
67      DUUI = DU1/DU0
68      DELU0 = -U(1)/DUUI

```

```

69      IF(UDIF.LT.0.0) U1L = U10
70      IF(UDIF.GT.0.0) U1R = U10
71      U10 = U10+DELU0
72      IF(U10.GT.U1R)U10=(U10-DELU0+U1R)/2.0
73      IF(U10.LT.U1L) U10 = (U10-DELU0 +U1L)/2.0
74      IF(ICOUNT.EQ.0) U10 = 0.5*(U1L+U1R)
75      DU0 = U10-U0OLD
76      ICOUNT = ICOUNT+1
77      IF(ICOUNT.LE.10) GO TO 5
78      TERM = U(1)*DX*X
79      40 CONTINUE

C
C      FOLLOWING SOLUTION OF PROBLEMS (1) AND (2) FOR THE WEIGHTING FUNCTION,
C      AXIAL POTENTIAL, AND AXIAL FLUX DISTRIBUTIONS, CALCULATE THE
C      DIMENSIONLESS CONDUCTIVITY, THE EFFECTIVE CONDUCTANCE, AND THE EFFEC-
C      TIVE SOIL WATER POTENTIAL.
C

80      U1P = U1P/U11S
81      SCAHOK = U1P
82      SCACON = -1.0/U(2)
83      SCAH = SCAHOK*SCACON
84      PHIINT = 1./SCAH
85      SCAHB = SCACON*RESFAC
86      HNUINT = U1P/RESFAC
87      GO TO 45
88      44 HOM = 1.0
89      N = KPT
90      GO TO 1
91      45 CONTINUE
92      M = KPT
93      DO 50 I=1,N
94      U1(I) = U1(I)/U11S
95      W(I) = W(I)/HNUINT
96      50 CONTINUE
97      DO 55 I=1,M
98      Q(I) = Q(I)/Q(M)
99      55 CONTINUE

C
C      CALCULATE ZERO-FLUX POINT AND MAXIMUM AXIAL POTENTIAL.
C

100     ZERO = STAR(XS1,Q,PHIX,M,X1,X2,PSTAR)
101     ZER = ZERO
102     PH1 = PSTAR

C
C      CHECK RESULTS FOR A CONSTANT TRANSFER COEFFICIENT DISTRIBUTION.
C

103     CK = CHECK(XS1,PHIX,RESFAC,M)

C
104     CALL OUTPUT

C
105     STOP
106     END

C      *
C
C      *
C
C      THE FUNCTION PHIS CALCULATES OR OTHERWISE
C      SUMMONS THE DIMENSIONLESS SOIL WATER PO-
C      TENTIAL CORRESPONDING TO THE CURRENT VAL-
C      UE OF X SUPPLIED TO IT FROM THE CALLING
C      PROGRAM. I/O STATEMENTS MUST BE SUPPLIED

```

```

C           IF DATA IS TO BE FED IN FOR THE COMPUTATION.
C
C           *
C           *
C

```

```

107      FUNCTION PHIS(X)
108      PHIS = X
109      RETURN
110      END

```

```

-----
-----

```

```

111      FUNCTION RUNGE(N,Y,F,X,DX)

```

```

-----
-----

```

```

C           SEE P.374 OF CARNAHAN ET AL., 1969
C
C           *
C           *
C
C           THE FUNCTION RUNGE INTEGRATES THE VECTOR
C           F ACROSS A STEP OF LENGTH H IN THE INDEPEND-
C           ENT VARIABLE X. VALUES OF F ARE SUPPLIED
C           FROM THE CALLING PROGRAM. THESE VALUES
C           CORRESPOND TO THE DERIVATIVES OF THE VEC-
C           TOR Y. VALUES OF Y AT X+H ARE THE PRODUCT
C           OF COMPUTATIONS OVER A FULL STEP. ONE
C           STEP REQUIRES FIVE PASSES THROUGH RUNGE
C           AND FOUR EVALUATIONS OF EACH COMPONENT
C           OF F BY THE CALLING PROGRAM.
C
C           *
C           *
C

```

```

112      INTEGER RUNGE
113      DATAM/0/
114      DIMENSION PHI(100),SAVEY(100),Y(N),F(N)
115      M = M+1
116      GO TO (1,2,3,4,5),M
117      1 RUNGE = 1
118      RETURN
119      2 DO 22 J=1,N
120      SAVEY(J) = Y(J)
121      PHI(J) = F(J)
122      22 Y(J) = SAVEY(J)+0.5*DX*F(J)
123      X = X+0.5*DX
124      RUNGE = 1
125      RETURN
126      3 DO 33 J=1,N
127      PHI(J) = PHI(J)+2.0*F(J)
128      33 Y(J) = SAVEY(J)+0.5*DX*F(J)
129      RUNGE = 1
130      RETURN
131      4 DO 44 J=1,N
132      PHI(J) = PHI(J)+2.0*F(J)
133      44 Y(J) = SAVEY(J)+DX*F(J)
134      X = X+0.5*DX
135      RUNGE = 1
136      RETURN
137      5 DO 55 J=1,N
138      55 Y(J) = SAVEY(J) + (PHI(J)+F(J))*DX/6.0
139      M = 0
140      RUNGE = 0
141      RETURN
142      END

```



```

143      FUNCTION STAR(XS1,Q,PHIX,M,X1,X2,PSTAR)
      C
      C          *
      C
      C          THE FUNCTION STAR PROVIDES A CUBIC INTER-
      C          POLATION ESTIMATE OF THE ZERO-FLUX POINT
      C          (STAR) AND THE MAXIMUM AXIAL POTENTIAL
      C          (PSTAR) ALONG THE AXIAL FLOW PATHWAY.
      C
      C          THE COEFFICIENTS IN THE INTERPOLATING
      C          POLYNOMIAL AND THEIR CORRESPONDING TERM
      C          EXPONENTS ARE AS FOLLOWS: COFA(0),
      C          COFB(1), COFC(2),COFD(3).
      C
      C          THE INTERVAL OVER WHICH THE FLUX CHANGES
      C          SIGN IS FIRST IDENTIFIED. THE COEFFICIENTS
      C          ARE DETERMINED TO INSURE AGREEMENT BETWEEN
      C          FUNCTION VALUES AND POLYNOMIAL VALUES
      C          AND BETWEEN DERIVATIVE VALUES OF THE FUNC-
      C          TION AND THE POLYNOMIAL AT BOTH END-POINTS
      C          OF THE INTERVAL.
      C
      C          *
      C
144      DIMENSION XS1(100),Q(100),PHIX(100)
145      RATIO = 1.0
146      STAR = 10.0
147      MM1 = M-1
148      DO 901 I=1,MM1
149      IP1 = I+1
150      QS1 = Q(I)
151      QS2 = Q(IP1)
152      IF(QS1.EQ.0.0) STAR = XS1(I)
153      IF(QS1.NE.0.0) RATIO = QS2/QS1
154      IF(RATIO.LT.0.0) GO TO 902
155      901 CONTINUE
156      902 IF(RATIO.EQ.1.0) STAR = 0.0
157      IF(RATIO.GT.0.0) GO TO 910
158      X1 = XS1(I)
159      X2 = XS1(IP1)
160      Y1 = PHIX(I)
161      Y2 = PHIX(IP1)
162      Y1P = -QS1
163      Y2P = -QS2
164      DS = X2-X1
165      DS2 = DS*DS
166      DY = Y2-Y1
167      DYDS = DY/DS
168      GAMA1 = Y1
169      GAMA2 = DYDS
170      GAMA3 = (DYDS-Y1P)/DS
171      GAMA4 = (Y1P+Y2P-2.0*DYDS)/DS2
172      SPL = X1+X2
173      S2 = X1*X1
174      S3 = S2*X1
175      S1 = X1
176      S2PL = S2+X2*SPL
177      COFD = GAMA4
178      COFC = GAMA3-COFD*(S1+SPL)
179      COFB = GAMA2-SPL*COFC-S2PL*COFD
180      COFA = Y1-S1*COFB-S2*COFC-S3*COFD
181      COFD3 = 3.0*COFD
182      IF(COFD3.EQ.0.0) GO TO 910
183      BNORM = 2.*COFC/COFD3
184      CNORM = COFB/COFD3
185      BNORM2 = BNORM*BNORM

```

```

186      DNORM = BNORM2-4.0*CNORM
187      IF(DNORM.LT.0.0) GO TO 910
188      SDNORM = SQRT(DNORM)
189      STAR1 = (SDNORM-BNORM)/2.0
190      STAR2 = -(SDNORM+BNORM)/2.0
191      IF(STAR1.LE.X2.AND.STAR1.GE.X1) STAR = STAR1
192      IF(STAR2.LE.X2.AND.STAR2.GE.X1) STAR = STAR2
193      PSTAR = COFA+STAR*(COFB+STAR*(COFC+STAR*COFD))
194  910 CONTINUE
195      IF(STAR.GT.1.0) STAR = 0.0
196      IF(STAR.EQ.0.0) PSTAR=PHIX(1)
197      RETURN
198      END

199      FUNCTION CHECK(XS1,PHIX,RESFAC,M)
C
C      *
C
C      THE FUNCTION CHECK CALCULATES DIMENSION-
C      LESS AXIAL POTENTIAL AT EACH POINT FOR
C      WHICH A CALCULATION OF POTENTIAL WAS MADE
C      USING THE RUNGE-KUTTA TECHNIQUE.
C
C      THE CALCULATION OF THE CHECK VALUES ARE
C      BASED ON THE ANALYTICAL SOLUTION TO THE
C      AXIAL FLOW PROBLEM FOR HN=1.
C
C      PHICHK IS THE CALCULATED POTENTIAL AND
C      DIFCHK IS THE DIFFERENCE BETWEEN PHICHK
C      AND PHIX, WHICH IS THE POTENTIAL VALUE
C      SUPPLIED FROM THE MAIN PROGRAM.
C
C      RESFAC IS THE RADIAL TO AXIAL TOTAL CON-
C      DUCTANCE RATIO.
C
C      COMPARISONS ARE ONLY VALID WHEN A CONSTANT
C      (HN=1) TRANSFER COEFFICIENT DISTRIBUTION
C      IS USED.
C
C      *
C
200      DIMENSION XS1(100),PHIX(100),DIFCHK(100),PHICHK(100)
201      BETA = SQRT(RESFAC)
202      TANBB = TANH(BETA)/BETA
203      BETI = 1./BETA
204      COB = COSH(BETA)
205      SOB = SINH(BETA)
206      DOB = BFTI*BETI/COB
207      BSOB = BETA*SOB
208      TERM = 1.0+BSOB-COB
209      CHKMOM = TERM*DOB
210      CHKSIG = TERM/BSOB
211      DO 60 I=1,M
212      X = XS1(I)
213      BX = BETA*X
214      BMX = BETA-BX
215      TER1 = COSH(BX)
216      TER2 = COSH(BMX)
217      TER3 = SINH(BX)
218      TER4 = SINH(BMX)
219      TER6 = TER1*(X*TER2-1.0)
220      TER7 = TER4*(X*TER3+BETI)
221      PHICHK(I) = (TER6+TER7)/COB
222      DIFCHK(I) = PHIX(I)-PHICHK(I)

```

```

223      60 CONTINUE
224      CHECK = 0.0
225      RETURN
226      END

227      FUNCTION HNORM(X,NFUN,HMOM,SIGH)
      C
      C
      C*      *
      C      * THE FUNCTION HNORM EVALUATES A TRANSFER
      C      * COEFFICIENT DISTRIBUTION DEFINED ON THE
      C      * UNIT INTEVERVAL. THE FUNCTION IS IDEN-
      C      * TIFIED BY THE CURRENT VALUE OF NFUN AND
      C      * IS EVALUATED AT THE CURRENT X-VALUE.
      C      * X AND NFUN ARE SUPPLIED BY THE CALLING
      C      * PROGRAM. THE FUNCTION VALUE IS RETURNED
      C      * AS HNORM. SIGH IS THE DISTRIBUTION-
      C      * WEIGHTED VALUE OF X.
      C*      *
      C
228      BHORN = 1.0/(140.*140.)
229      IF(X.EQ.0.0) IND = 0
230      GO TO (1,2,3,4,5,6,7),NFUN
231      1 IF(IND.GT.0) GO TO 11
232      10 CONTINUE
      C
      C*      *
      C
      C      NFUN = 1
      C
      C      INVERSE HYPERBOLIC SINE
      C
233      T1 = 1.+BHORN
234      T2 = SQRT(T1)
235      T5 = SQRT(BHORN)
236      T6 = 1.+T2
237      HMOM = 0.25*(BHORN*ALOG(T5/T6)+T2)
238      SIGB = HMOM/(T2-T5)
239      IND = 1
240      11 IF(NFUN.EQ.2) GO TO 2
241      SIGH = SIGB
242      XS = X
243      GO TO 22
      C
244      2 IF(IND.EQ.0) GO TO 10
245      SIGH = 1.-SIGB
246      XS = X
      C
      C*      *
      C      *
      C      NFUN = 2
      C
      C      ROTATED INVERSE HYPERBOLIC SINE
      C
247      X = 1.-X
248      22 T3 = X**2+BHORN
249      T4 = SQRT(T3)
250      T7 = X+T4
251      HNORM = ALOG(T6/T7)/(T2-T5)
      C
      C*      *
      C
252      X = XS
253      RETURN

```

```

C
C*      *
C      NFUN = 3
C
C      EXPONENTIAL
254      3 IF(IND.NE.0) GO TO 31
255      30 CONTINUE
256      A = -4.6
257      C = EXP(A)
258      D = 4.6/(1.-C)
259      SIGB = (1.0-5.6*C)/4.6
260      HMOM = SIGB/4.6
261      IND = 1
262      IF(NFUN.EQ.4) GO TO 4
263      31 B = A*X
264      SIGH = SIGB
265      E = EXP(B)
266      HNORM = E*D
267      RETURN
268      4 IF(IND.EQ.0) GO TO 3
269      XS = X

C
C*      *
C
C      NFUN = 4
C
C      ROTATED EXPONENTIAL
271      X = 1.-X
272      SIGH = 1.-SIGB
273      B = A*X
274      E = EXP(B)
275      HNORM = E*D
276      X = XS
C*      *
277      RETURN
278      6 CONTINUE

C
C*      *
C      NFUN = 5
C
C      LINEAR
279      5 HMOM = 1.0/6.0
280      SIGB = 1.0/3.0
281      XS = X
282      SIGH = SIGB
C*      *
C      NFUN = 6
C
C      ROTATED LINEAR
C*      *
283      IF(NFUN.EQ.6) X=1.-X
284      IF(NFUN.EQ.6) SIGH = 1.-SIGB
C*      *
285      HNORM = 2.0*(1.-X)
C
C*      *
286      X = XS
287      IND = 1
288      RETURN

C
C*      *
C      NFUN = 7
C
C      CONSTANT

```

C

```

289       7 CONTINUE
290         HMOM = 0.5
291         SIGH = 0.5
292         HNORM = 1.0
C*      *
293       IND = 1
294       RETURN
295       END

296       SUBROUTINE OUTPUT
297       COMMON N,M,NFUN,SCACON,SCAH,PHIINT,RESFAC,ZER,PHI,HNUINT,SIGH
298       COMMON PHIX,PHIST,Q,HN,W,XS,XS1,U1,ERROR
299       DIMENSION PHIX(100),PHIST(100),Q(100),HN(100),W(100),XS(100)
300       DIMENSION XS1(100),U1(100)
301       WRITE(6,200)
302       200 FORMAT(1H1/25X,'SOLUTION TO THE NORMALIZED LINEAR FLOW SYSTEM'//
303         I 25X,'D(DY/DX)/DX - B*Y = PHI'//25X,'DY/DX(0) = 0; Y(1) = 0')
304       WRITE(6,290)
305       290 FORMAT(//25X,'B = H*L**2/K; Y = PHIX, THE AXIAL POTENTIAL')
306       222 FORMAT(///25X,' THE DIFFERENCE IN CALCULATED AND ACTUAL VALUES OF
307         I THE BOUNDARY CONDITION AT X = 1 IS'//)
308       WRITE(6,223) ERROR
309       223 FORMAT(25X,'LESS THAN ',F8.4,' IF ICOUNT IS NO GREATER THAN 10')
310       WRITE(6,202)
311       202 FORMAT(/10X,' U = SOLUTION TO AUXILLARY SYSTEM')
312       WRITE(6,203)
313       203 FORMAT(/10X,' W = NORMALIZED WEIGHTING FUNHCTION')
314       WRITE(6,204)
315       204 FORMAT(/10X,' HN = DIMENSIONLESS TRANSFER COEFFICIENT')
316       WRITE(6,205)
317       205 FORMAT(/10X,' PHIX = DIMENSIONLESS AXIAL POTENTIAL')
318       WRITE(6,206)
319       206 FORMAT(/10X,' PHI = DIMENSIONLESS SOIL WATER POENTIAL')
320       WRITE(6,207)
321       207 FORMAT(/10X,' Q = DIMENSIONLESS AXIAL FLUX')
322       WRITE(6,250)
323       250 FORMAT(1H1)
324       WRITE(6,201) RESFAC
325       201 FORMAT(///25X,'H*L**2/K = ',F10.4//)
326       WRITE(6,80)
327       IF(NFUN.EQ.1) WRITE(6,81)
328       IF(NFUN.EQ.2) WRITE(6,82)
329       IF(NFUN.EQ.3) WRITE(6,83)
330       IF(NFUN.EQ.4) WRITE(6,84)
331       IF(NFUN.EQ.5) WRITE(6,85)
332       IF(NFUN.EQ.6) WRITE(6,86)
333       IF(NFUN.EQ.7) WRITE(6,87)
334       80 FORMAT(///25X,'THE TRANSFER COEFFICIENT DISTRIBUTION IS')
335       81 FORMAT(//25X,'HORN'//)
336       82 FORMAT(//25X,' ROTATED HORN'//)
337       83 FORMAT(//25X,' EXPONENTIAL'//)
338       84 FORMAT(//25X,' ROTATED EXPONENTIAL'//)
339       85 FORMAT(//25X,' LINEAR'//)
340       86 FORMAT(//25X,' ROTATED LINEAR'//)
341       87 FORMAT(//25X,' CONSTANT'//)
342       WRITE(6,208) (XS(I),I=1,N)
343       208 FORMAT(/ 5X,'X = ',15F8.3)
344       WRITE(6,208) (XS1(I),I=1,M)
345       WRITE(6,209)(U1(I),I=1,N)
346       209 FORMAT(/ 5X,'U = ',15F8.3)
347       WRITE(6,210)(W(I),I=1,N)
348       210 FORMAT(/ 5X,'W = ',15F8.3)
349       WRITE(6,211) ( HN(I),I=1,N)

```

```
349 211 FORMAT(/ 5X,'HN = ',15F8.3)
350     WRITE(6,212) (PHIX(I),I=1,M)
351 212 FORMAT(/ 3X,'PHIX = ',15F8.3)
352     WRITE(6,213)(PHIST(I),I=1,M)
353 213 FORMAT(/ 3X,'PHIS = ',15F8.3)
354     WRITE(6,214) (Q(I),I=1,M)
355 214 FORMAT(/ 5X,'Q = ',15F8.3)
356     WRITE(6,215)
357 215 FORMAT(///36X,'DIMENSIONLESS VARIABLES'//)
358     WRITE(6,216)
359 216 FORMAT(5X,'CONDUCTIVITY',10X,'EFFECTIVE SYSTEM CONDUCTANCE',10X,
1'EFFECTIVE SOIL WATER POTENTIAL'/)
360     WRITE(6,217) SCACON,SCAH,PHIINT
361 217 FORMAT(5X,F10.4,12X,F10.4,28X,F10.4)
362     WRITE(6,218)
363 218 FORMAT(//5X,'ZERO FLUX POINT',10X,'MAX POTENTIAL',10X,'INTEGRAL OF
1HN*U',10X,'MEAN X FOR HN'/)
364     WRITE(6,219) ZER,PH1,HNUINT,SIGH
365 219 FORMAT(5X,F10.4,15X,F10.4,13X,F10.4,16X,F10.4//)
366     RETURN
367     END
```

\$ENTRY

SOLUTION TO THE NORMALIZED LINEAR FLOW SYSTEM

$$D(DY/DX)/DX - B*Y = PHI$$

$$DY/DX(0) = 0; Y(1) = 0$$

$$B = H*L**2/K; Y = PHIX, THE AXIAL POTENTIAL$$

THE DIFFERENCE IN CALCULATED AND ACTUAL VALUES OF THE BOUNDARY CONDITION AT X = 1 IS
LESS THAN 0.0002 IF ICOUNT IS NO GREATER THAN 10

U = SOLUTION TO AUXILLARY SYSTEM

W = NORMALIZED WEIGHTING FUNCTION

HN = DIMENSIONLESS TRANSFER COEFFICIENT

PHIX = DIMENSIONLESS AXIAL POTENTIAL

PHI = DIMENSIONLESS SOIL WATER POTENTIAL

Q = DIMENSIONLESS AXIAL FLUX

H*L**2/K = 0.1000

THE TRANSFER COEFFICIENT DISTRIBUTION IS

HORN

X =	0.000	0.100	0.200	0.300	0.400	0.500	0.600	0.700	0.800	0.900	1.000
X =	0.000	0.100	0.200	0.300	0.400	0.500	0.600	0.700	0.800	0.900	1.000
U =	0.929	0.931	0.935	0.941	0.947	0.955	0.963	0.972	0.981	0.991	1.000
W =	1.496	0.612	0.430	0.324	0.248	0.189	0.141	0.099	0.063	0.030	0.000
HN =	5.675	2.318	1.621	1.212	0.923	0.698	0.514	0.359	0.225	0.106	0.000
PHIX =	0.013	0.013	0.013	0.012	0.011	0.010	0.009	0.007	0.005	0.002	0.000
PHIS =	0.000	0.100	0.200	0.300	0.400	0.500	0.600	0.700	0.800	0.900	1.000
Q =	0.000	0.040	0.148	0.285	0.434	0.581	0.716	0.832	0.922	0.980	1.000

DIMENSIONLESS VARIABLES

CONDUCTIVITY

41.7256

EFFECTIVE SYSTEM CONDUCTANCE

3.9576

EFFECTIVE SOIL WATER POTENTIAL

0.2527

ZERO FLUX POINT

0.0000

MAX POTENTIAL

0.0130

INTEGRAL OFHN*U

0.9485

MEAN X FOR HN

0.2517

STATEMENTS EXECUTED= 7062

CORE USAGE OBJECT CODE= 16240 BYTES,ARRAY AREA= 6100 BYTES,TOTAL AREA AVAILABLE= 126976 BYTES

DIAGNOSTICS NUMBER OF ERRORS= 0, NUMBER OF WARNINGS= 0, NUMBER OF EXTENSIONS= 3

COMPILE TIME= 0.16 SEC,EXECUTION TIME= 0.07 SEC, 20.46.11 THURSDAY 3 MAR 83 WATFIV - MAR 1980 V2L0

Appendix E

Notes On A Qualitative Analysis Of The Radial-Axial Flow System For $\bar{k}_x(\sigma) = \bar{k}_x^*$

Introduction

The flow model under consideration is applicable to water transport in soil-root systems. The model is based on integral solutions of a two point boundary value problem (Equations 6-6b) derived from assumptions of linear, steady, radial-axial flow. Water absorption into a root system is assumed to be proportional to the difference between the bulk soil water potential $\psi_s(y)$ and the xylem water potential $\psi_x(y)$, where y is the distance, along an axial pathway. (For a path of length L , the distance of a point from the outflow boundary is $L-y$.) Water flux in the root vascular system is assumed to be proportional to the xylem potential gradient $d\psi_x/dy$. The radial transfer coefficient, $h(y)$, governs absorption, and the axial conductivity, $k_x(y)$, governs transport in the root xylem. A general solution to the problem was obtained by a Green's function technique, and it was shown that the solution leads to three system functions: the system distribution constant, $D_{h,k}$, the dimensionless effective soil water potential Ψ_s , and the effective system conductance, H . The equation

$$\bar{H} \Psi_s = 1$$

is obeyed in the dimensionless system, and back-transforms to the equation:

$$H (\Psi_s - \psi_o) = q_o,$$

where H is the effective system conductance, Ψ_s is the effective soil water potential, ψ_o is the xylem water potential at the outflow boundary ($y = L$) and q_o is the flux at the outflow boundary, of the original dimensional system.

It was shown that the dimensionless effective soil water potential is the weighted mean of $\bar{\psi}_s(\sigma)$ over the flow region:

$$\Psi_s = \int_0^1 \bar{w}(\sigma) \bar{\psi}_s(\sigma) d\sigma,$$

where the weighting function is

$$\bar{w}(\sigma) = \bar{h}_n(\sigma) \cdot \bar{u}_1(\sigma) / D_{h,k}.$$

The distribution constant $D_{h,k}$ is:

$$D_{h,k} = \int_0^1 \tilde{h}_n(\sigma) \tilde{u}_1(\sigma) d\sigma$$

where $\tilde{h}_n(\sigma)$ is the normalized transfer coefficient. In the integrand of the above expression, $\tilde{u}_1(\sigma)$ is the solution of the homogeneous equation which satisfies the two boundary conditions

$$\tilde{u}_1'(0) = 0$$

and

$$\tilde{u}_1(1) = 1$$

The function $\tilde{u}_1(\sigma)$ can be interpreted as the dimensionless axial potential distribution that would accompany a reverse flow with the potential at the outflow boundary equal to 0, and the soil water potential uniformly equal to ψ_0 for $0 \leq y \leq L$. It can be shown that $\tilde{u}_1(\sigma)$ is a non-decreasing function over $0 \leq \sigma \leq 1$, and due to the boundary conditions it is non-negative. Since $\tilde{h}_n(\sigma)$ only reflects the distribution of the transfer coefficient function, $h(y)$, and not its magnitude, $D_{h,k}$ is a parameter whose magnitude depends on the spatial distribution of $h(y)$ but does not depend on the magnitude of $h(y)$.

In the case where both the axial conductivity, $k_x(y)$ and the radial transfer coefficient, $h(y)$, are constant functions, the following observations hold. First, the radial transfer coefficient is given by $h(y) = h^*$. The corresponding dimensionless transfer coefficient is therefore $\tilde{h}(\sigma) = \tilde{h}^*$ and the transfer coefficient distribution is $\tilde{h}_n(\sigma) = 1$. Secondly, the axial conductivity is $k_x(y) = k_x^*$. So from equation $\beta^{*2} = h_T/k_x(1) = h^*/k^*$. The auxiliary potential function in this case is $\tilde{u}_1(\sigma) = \cosh(\beta^*\sigma)/\cosh \beta^*$, which is an increasing function of σ for any $\beta^* > 0$. The distribution constant is

$$D_{h,k}^* = \int_0^1 \cosh \beta^*\sigma d\sigma / \cosh \beta^*$$

or

$$D_{h,k}^* = \tanh \beta^* / \beta^*$$

Of particular interest is the behavior of $D_{h,k}$ as $h^*/k^* = \beta^{*2}$ approaches 0. L' Hospital's rule applied to the above expression gives

$$\lim_{\beta^* \rightarrow 0} D_{h,k}^* = 1$$

Moreover, $\lim_{\beta^* \rightarrow 0} \tilde{u}_1(\sigma) = \lim_{\beta^* \rightarrow 0} \cosh(\beta^*\sigma)/\cosh \beta^* = 1$,

and the convergence is uniform on the interval $0 \leq \sigma \leq 1$. Since the weighting function $\tilde{w}(\sigma) = \tilde{h}_n(\sigma) \tilde{u}_1(\sigma) / D_{h,k}^*$, and since in this case $\tilde{h}_n(\sigma) = 1$, $\tilde{w}(\sigma)$ is also an increasing function of σ for any particular value of β^* and finally,

$$\lim_{\beta^* \rightarrow 0} \tilde{w}(\sigma) = 1$$

The convergence of $\bar{w}(\sigma)$ to 1 is uniform on $0 \leq \sigma \leq 1$. Therefore

$$\lim_{\beta^* \rightarrow 0} \bar{\Psi}_s = \lim_{\beta^* \rightarrow 0} \int_0^1 \bar{w}(\sigma) \bar{\psi}_s(\sigma) d\sigma = \int_0^1 \bar{\psi}_s(\sigma) d\sigma.$$

The implication is that, for constant flow controlling parameters, the soil water potential that is "effective" in the sense of an Ohm's Law equation, approaches the spatial mean value of the soil water potential, as the ratio of the constant radial transfer coefficient to the constant axial conductivity approaches 0. Since $\bar{w}(\sigma) = \beta^* \cosh(\beta^* \sigma) / \sinh \beta^*$, for this special case we have $\bar{w}(0) = \beta^* \operatorname{csch} \beta^*$. In conclusion, as β^* increases from 0 to 1, $\bar{w}(\sigma)$ decreases from 1.000 to 0.851 while $\bar{w}(1)$ increases from 1.000 to 1.313. For any fixed value of L , these trends reflect the heavier weighting imparted to potentials near the outflow boundary ($\sigma = 1$) with increases in the ratio of the radial transfer coefficient to the axial conductivity.

Nature of the Qualitative Analysis

The present study was carried out to study the system for a variable transfer coefficient. A series of twenty-eight computer runs was conducted with a program designed to solve the radial-axial flow problem (6) – (6b), under the further restriction $k_x(y) = k_x^*$. With this assumption the original problem can be rewritten in the form (D-1) – (D-1b), in which it is clear that the principle system controlling variables are the radial-to-axial conductance ratio $\beta^{*2} = h_T/k_x(1) = h_T/k_x^*$, and the dimensionless transfer coefficient distribution, $\bar{h}_n(\sigma)$. In a corresponding dimensional system β^{*2} is equivalent to $L \int_0^L h(y) dy / k_x^*$ and $\bar{h}_n(\sigma)$ is equivalent to $L h(y) \int_0^L h(y) dy$, where $h(y)$ is the transfer coefficient distribution in the dimensional system.

The set of 28 runs was made with a single assumed soil water potential distribution, $\psi_s(y) = y$. It was previously indicated that this distribution leads to equality between the effective soil water potential and the first moment of the weighting function $\bar{\sigma}_w$. Seven different transfer coefficient distributions (Table E-1 and Figures E-1 and E-2) and four values of β^{*2} : (0.1, 0.4, 1.6, and 6.4) were used to generate the 28 runs. The $\bar{h}_n(\sigma)$ functions differ in their values at $\sigma = 0$ and $\sigma = 1$ and also in their first moments, $\bar{\sigma}_h$, which range from 0.205 to 0.795. With the exception of the constant function ($\bar{\sigma}_h = 0.5$), they are all strongly monomodel.

Table E-1.
Transfer Coefficient Distribution Functions,
Their Values at $\sigma = 0$ and $\sigma = 1$, and Their
First Moments, $\bar{\sigma}_h$

Function	$\tilde{h}_n(\sigma)$	$\tilde{h}_n(0)$	$\tilde{h}_n(1)$	$\bar{\sigma}_h$
1. Exponential	$4.6\bar{e}^{-4.6\sigma}/(1 - \bar{e}^{-4.6})$	4.650	0.047	0.205
2. Inverse Hyperbolic Sine	$[C_R(1) - C_R(0) - 1]^{-1} \cdot \ln [C_R(1)/C_R(\sigma)]^*$	5.680	0.000	0.250
3. Linear	$2(1 - \sigma)$	2.000	0.000	0.333
4. Constant	1	1.000	1.000	0.500
5. RL	— †	0.000	2.000	0.667
6. RIHS	— †	0.000	5.680	0.750
7. REXP	— †	0.047	4.652	0.795

* $C_R(\sigma) = \sigma + \sqrt{\sigma^2 + R^{-2}}$; $R = 140$.

†Expressions for 5, 6, and 7 are obtained by substituting $1 - \sigma$ for σ in the expressions for 1, 2, and 3, respectively.

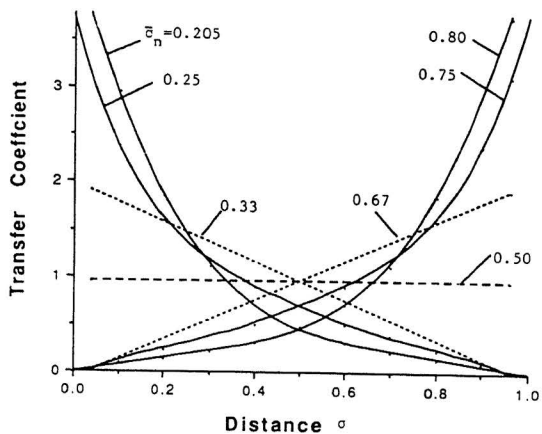


Fig. E-1 The Transfer Coefficient Distributions $\tilde{h}_n(\sigma)$ and Their $\bar{\sigma}_n$ Values

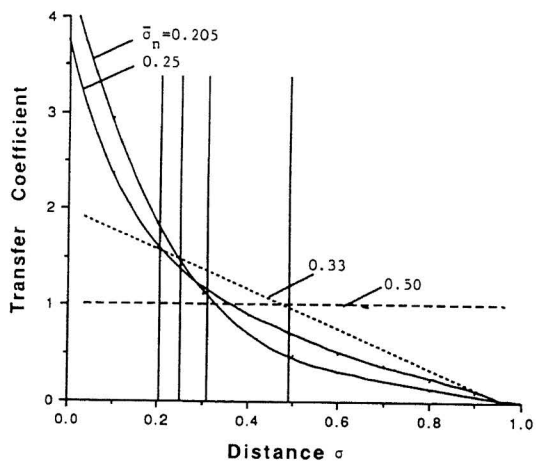


Fig. E-2 The Transfer Coefficient Distributions $\tilde{h}_n(\sigma)$ and Their $\bar{\sigma}_n$ Values

Discussion of Results of the Qualitative Analysis

Graphs of the computed dimensionless flux $\tilde{q}_x(\sigma)$ (curved dashed line) and the dimensionless axial potential $\tilde{\psi}_x(\sigma)$ (solid line with asterisks) are shown in Figures E-3 through E-14. The dashed straight line represents the soil water potential, $\tilde{\psi}_s(y) = y$, which was the same for all of the runs made. The $\tilde{\psi}_x$ function values indicated by asterisks were computed using Jung's (1980) lumped resistance algorithm.

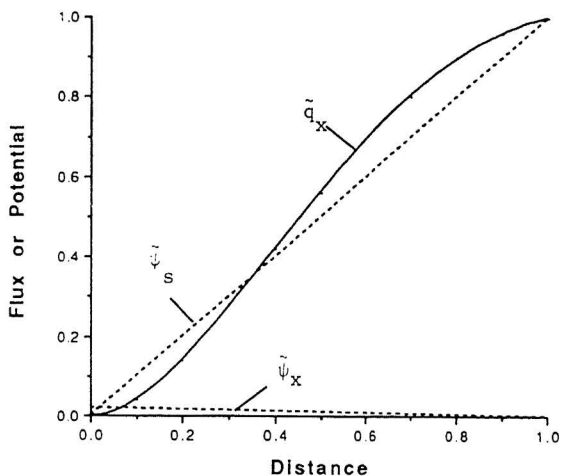


Fig.E-3 Dimensionless Axial Flow
Variables $\beta^{*2}=0.10$, $\tilde{\sigma}_h=0.25$

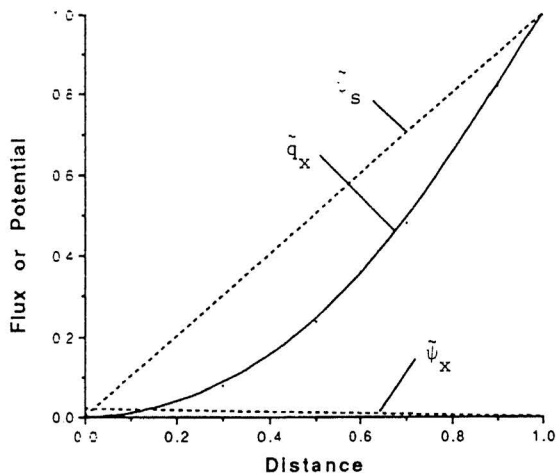


Fig.E-4 Dimensionless Axial Flow
Variables $\beta^{*2}=0.10$, $\tilde{\sigma}_h=0.50$

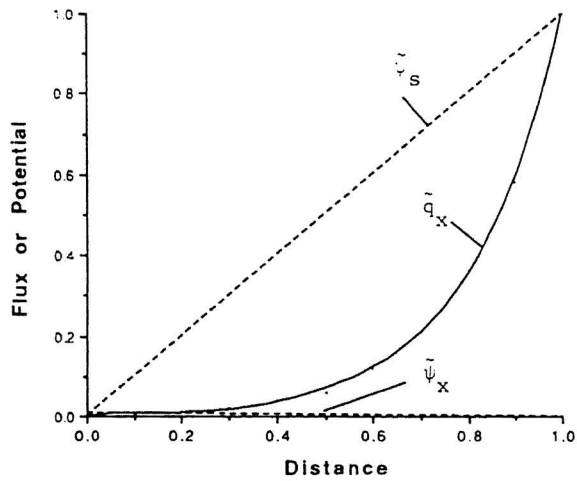


Fig.E-5 Dimensionless Axial Flow
 Variables $\beta^{*2}=0.10$, $\bar{c}_h=0.75$

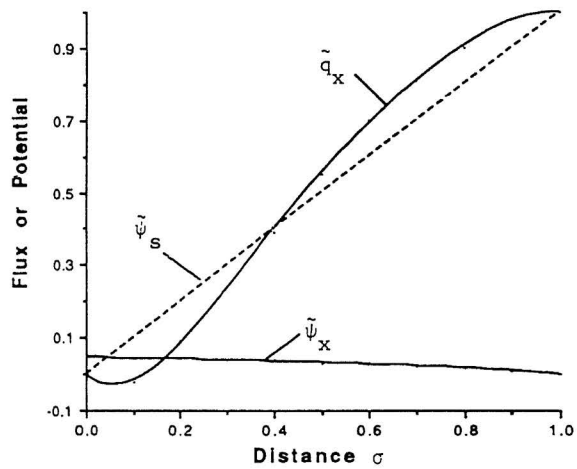


Fig.E-6 Dimensionless Axial Flow
 Variables $\beta^{*2}=0.40$, $\bar{c}_h=0.25$

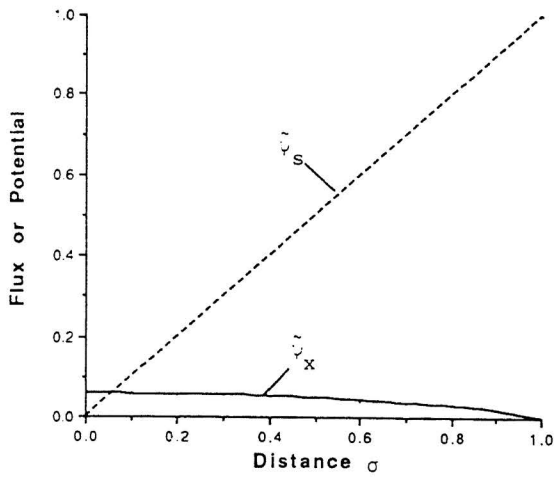


Fig.E-7 Dimensionless Axial Flow
Variables $\beta^* \approx 0.40$, $\bar{\sigma}_h = 0.50$

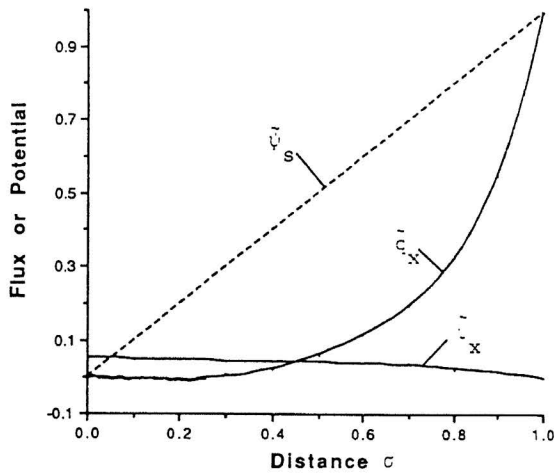


Fig.E-8 Dimensionless Axial Flow
Variables $\beta^* = 0.40$, $\bar{\sigma}_h = 0.75$

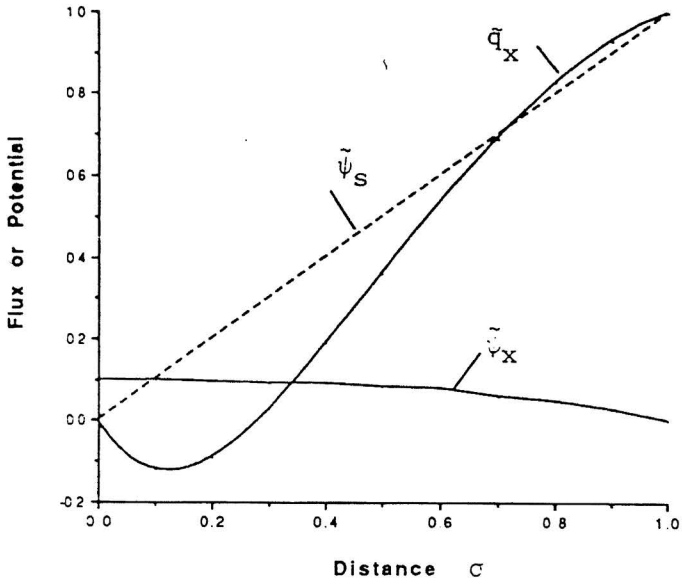


Fig.E-9 Dimensionless Axial Flow
 Variables $\beta^* \approx 1.6, \bar{\sigma}_h = 0.25$

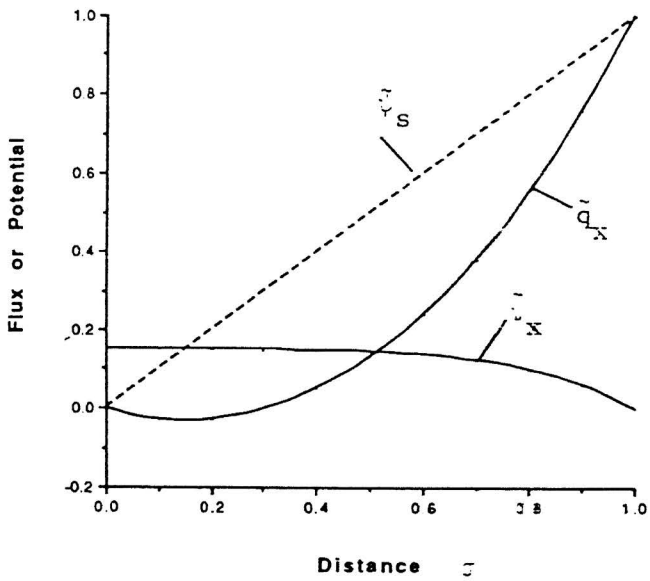


Fig.E-10 Dimensionless Axial Flow
 Variables $\beta^* \approx 1.6, \bar{\sigma}_h = 0.50$

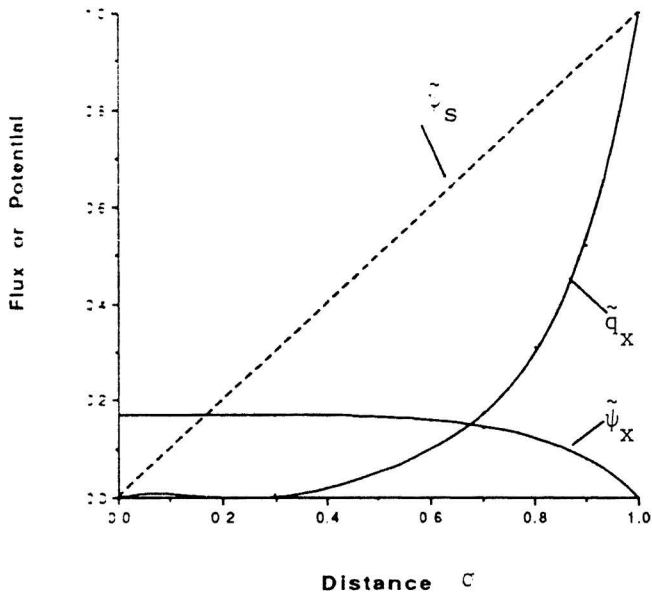


Fig.E-11 Dimensionless Axial Flow
 Variables $\beta^* = 1.6$, $\tilde{\sigma}_h = 0.75$

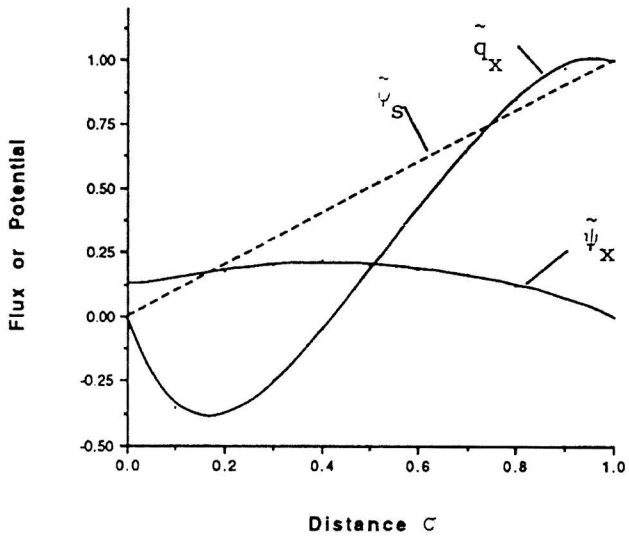


Fig.E-12 Dimensionless Axial Flow
 Variables $\beta^* = 6.4$, $\tilde{\sigma}_h = 0.25$

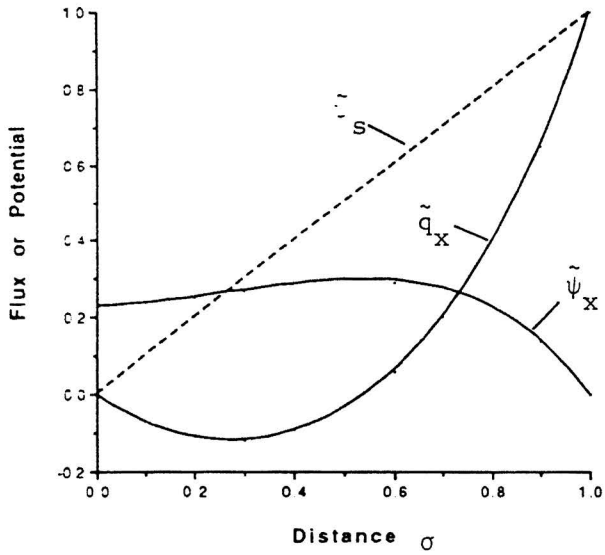


Fig.E-13 Dimensionless Axial Flow
 Variables $\beta^* = 6.4$, $\tilde{\sigma}_h = 0.5$

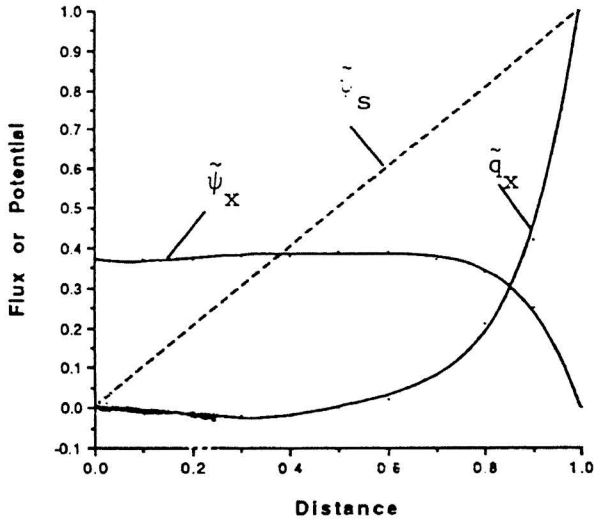


Fig.E-14 Dimensionless Axial Flow
 Variables $\beta^* = 6.4$, $\tilde{\sigma}_h = 0.75$

Preliminary Observations Relevant to Interpretation of the Graphs

- (1) The flow equation (D-1) shows that β^{*2} and $\tilde{h}_n(\sigma)$ are independent with respect to their influences on all of the computed quantities considered in the analysis. However,
 - a. The system distribution constant $D_{h,k}$ depends explicitly on $\tilde{h}_n(\sigma)$ and $\tilde{u}_1(\sigma)$ in equation (36). The function $\tilde{w}(\sigma)$ depends on both $\tilde{h}_n(\sigma)$ and β^{*2} , by virtue of the fact that \tilde{u}_1 solves the auxillary flow equation (6 - c). Therefore, both $D_{h,k}$ and $\tilde{w}(\sigma)$ are expected to reflect changes made in either β^{*2} or $\tilde{h}_n(\sigma)$.
 - b. In the present study the chosen water potential distribution is such that $\tilde{\Psi}_s = \tilde{\sigma}_w$. The graphs presented are labeled with $\tilde{\sigma}_w$ instead of $\tilde{\Psi}_s$. The effective soil water potential, $\tilde{\Psi}_s$ is the integral of the product of $\tilde{w}(\sigma) = \tilde{h}_n(\sigma) \tilde{u}_1(\sigma)/D_{h,k}$ with $\tilde{\psi}_s(\sigma)$. This fact, together with the preceding remark implies that $\tilde{\Psi}_s$ must be affected by any changes made in β^{*2} , $\tilde{h}_n(\sigma)$ or $\tilde{\psi}_s(\sigma)$. However, since the same soil water potential distribution was used in all of the runs made, only the influences of β^{*2} and $\tilde{h}_n(\sigma)$ are manifested in the figures presented here.

- (2) The back-transformation of $\tilde{\psi}_s(\sigma) = \psi$ in the dimensional space frame is also linear: $\psi_s(y) = \psi_o(1 - y/L)$. Its maximum value is 0 at the outflow boundary, $y = L$, and its minimum value is equal to the outflow boundary axial potential, ψ_o . The back-transformed soil water potential takes on the value ψ_o at the position ($y = 0$) farthest from the outflow boundary. This aspect of the assumed soil water potential distribution influences the computed $\tilde{\psi}_x$ and \tilde{q}_x distributions illustrated in Figures E-3 through E-14, and is therefore relevant to any interpretation of the back-transformed distributions. Finally, it should be noted that this $\tilde{\psi}_s(\sigma)$ reflects a condition of increasing "dryness" with increasing distance from the outflow boundary.

Effects of β^{*2} and $\tilde{\sigma}_n$ on the $\tilde{\psi}_x$ and \tilde{q}_x Functions

Graphs of the dimensionless axial flux, \tilde{q}_x , and the dimensionless axial potential, $\tilde{\psi}_x$, are shown in Figures E-3 through E-14. For each of the figures, the independent variable plotted on the horizontal axis is the dimensionless distance $\sigma = y/L$, where L is the axial pathlength and y is the distance from the outer extremity of the axial pathway, where flux is 0. The value $\sigma = 1$ corresponds to the outflow boundary, where $\psi_x = \psi_o$ in the dimensional system. The dimensionless axial flux is, by definition, equal to 1 at $\sigma = 1$, since $\tilde{q}_x = q_x/q_o$ and $q_x(L) = q_o$. Similarly, $\tilde{\psi}_x(1) = 0$ since $\tilde{\psi}_x = (\psi_o - \psi_x)/\psi_o$ and $\psi_x(L) = \psi_o$. These values of $\tilde{q}_x(1)$ (curved dashed line) and $\tilde{\psi}_x(1)$ (solid line with asterisks) are common to all of the graphs. The straight dashed line, making a 45° angle with the positive

σ -axis on each of the figures, is the dimensionless soil water potential, $\tilde{\psi}_s(\sigma) = \sigma$.

Finally, there is a relatively flat region in all of the $\tilde{\psi}_x$ graphs near $\sigma = 0$ (Figures E-3 through E-14). This region reflects the no-flow boundary condition at $\tilde{\sigma} = 0$: $\tilde{\psi}'_x(0) = 0$. The uniformly higher values of $\tilde{\psi}_x$ at high β^{*2} (for example, Figure E-14) occur in conjunction with steeper gradients near the outflow boundary. One way to view this is that for a fixed value of the transfer coefficient, a higher value of β^{*2} would correspond to a lower axial conductivity. The total potential difference $\psi_s - \psi_o$, between the soil at any given position, along the pathway, and the outflow boundary, is partitioned between the axial and the radial segments of the pathway. Thus, $\psi_s - \psi_o = (\psi_s - \psi_x(y)) + (\psi_x(y) - \psi_o)$. The shift to a higher value of β^{*2} (lower value of k_x^*) is reflected in a corresponding shift of the above partitioning so that more of the total potential difference $\psi_s - \psi_o$ is due to $\psi_x - \psi_o$, and less to $\psi_s - \psi_x$. This shift accompanies steeper ψ_x gradients in the axial pathway near the outflow boundary which would serve to offset a lower k_x^* . The increasing ψ_x value and steepening gradients with increasing β^{*2} , are evident in Figures E-3, E-6, E-9, and E-12, for one of the transfer coefficient distributions studied.

Another trend in $\tilde{\psi}_x$ is the tendency of its graph to buckle at higher values of β^{*2} . This tendency occurs partly in association with the values of the dimensionless soil water potential, $\tilde{\psi}_s$, near $\sigma = 1$. The axial potential is maintained at 0 at $\sigma = 1$ in accord with the imposed boundary conditions. The ψ_x values increase a short distance upstream in response to the potential difference $\psi_s - \psi_x$ and the rate of increase of ψ_x with increasing distance from the outflow boundary is greater at higher values of β^{*2} . As the radial flux enters the axial pathway, it is partitioned into a positive component which exits via the outflow boundary in response to the negative potential gradient $d\tilde{\psi}_x/d\sigma$ for $\sigma > \sigma^*$ (flux-reversal point), and a negative component which reenters the soil upstream. This partitioning of the flux is hardly noticeable at low values of β^{*2} but is very evident at higher values. The soil water potential distribution would be expected to have appreciable bearing on the tendency toward development of these reverse flows, as well as on their magnitudes and positions.

The buckling effect of high β^{*2} on the $\tilde{\psi}_x$ graph is manifested differently in the \tilde{q}_x graph. For $\beta^{*2} = 0.1$, \tilde{q}_x appears to be non-negative, for all σ , as can be seen in Figures E-3 through E-5. As β^{*2} increases, a zone of $\tilde{q}_x < 0$ begins to be apparent and becomes more extensive and intense with further increases in β^{*2} . For $\beta^{*2} = 0.4$ and $\bar{\sigma}_h = 0.25$ the minimum value of \tilde{q}_x is less than -0.35 and the zone of negative \tilde{q}_x extends from $\sigma = 0$ to approximately $\sigma = 0.44$. The same trend in the \tilde{q}_x graphs also occurs for the other transfer coefficient distributions studied for this value of β^{*2} . However, the values of minimum flux and the extent and position of the zones of negative flux differ from those for $\bar{\sigma}_h = 0.25$. In each case the minimum flux corresponds to the point where the $\tilde{\psi}_x$ graph intersects the $\tilde{\psi}_s$ graph.

This is a result of the underlying flow assumption:

$$q'_x = \bar{h}(\sigma)(\bar{\psi}_x - \bar{\psi}_s)$$

At the point where $\bar{\psi}_x = \bar{\psi}_s$, $q'_x = 0$, separating the region where the flux is increasingly diminished with increasing σ , from the region where the flux is augmented with increasing σ . The flux corresponding to this point of intersection is the main increase over the region.

General Trends in $\bar{\psi}_s$ and \bar{q}_x with Increasing $\bar{\sigma}_h$

The dimensionless transfer coefficient $\bar{h}_n(\sigma)$ determines the spatial distribution of the absorption flux that would be associated with a constant potential difference $\bar{\psi}_s - \bar{\psi}_x$. It is a function which represents a continuously variable "gate" over the pathway. At points, σ , where $\bar{h}_n(\sigma)$ is relatively large, the rate of augmentation of q_x would also be relatively large in comparison to the rate of augmentation at other points under conditions of constant $\bar{\psi}_s - \bar{\psi}_x$. However, the chosen \bar{h}_n functions manifest an obvious "gate-type" influence on graphs of q_x in the figures. The first moment, $\bar{\sigma}_{h_1}$, of the \bar{h}_n distribution tends to track the gate position for the monomodal distributions studied. The influence on \bar{q}_x shows up as shifts in the position of steepest slope in the graph of \bar{q}_x which correspond to shifts in the value of $\bar{\sigma}_h$. The slope is steepest in the zone where the radial influx of water is most rapid, as is shown in the underlying flow equation

$$d\bar{q}_x/d\sigma = \bar{h}_T \bar{h}_n (\bar{\psi}_s(\sigma) - \bar{\psi}_x(\sigma))$$

For $\bar{\sigma}_h = 0.25$ and $\beta^{*2} = 0.10$, the position of steepest slope in the q_x graph (Figure E-3) is in the range $\sigma = 0.2$ to $\sigma = 0.4$. By comparison, for $\bar{\sigma}_h = 0.75$, the position of steepest slope is in the range 0.8 to 1.0. It can not be determined from the graphs where the position of maximum slope of q_x occurs for $\bar{\sigma}_h = 0.5$. It is clear, however, that the corresponding σ value is greater than the one for $\bar{\sigma}_h = 0.25$.

Another trend in the \bar{q}_x graph is that the minimum value of \bar{q}_x of such flow from tends to increase with increasing $\bar{\sigma}_h$. For $\beta^{*2} = 1.6$, for example, the minimum value of \bar{q}_x is approximately -0.14 for $\bar{\sigma}_h = 0.5$, and approximately 0.0 at $\bar{\sigma}_h = 0.75$. For $\beta^{*2} = 6.4$ the minimum value of q_x increases from -0.40 to -0.02 , as $\bar{\sigma}_h$ increases from 0.25 to 0.75.

The impact of variations in β^{*2} and $\bar{h}_n(\sigma)$ on properties of the $\bar{\psi}_x(\sigma)$ and $\bar{q}_x(\sigma)$ was considered in the preceding section. The first moment of the $\bar{h}_n(\sigma)$ distribution, $\bar{\sigma}_{h_1}$, was chosen as a parameter for reflecting differences among the particular set of $\bar{h}_n(\sigma)$ analyzed. We will conclude the discussion by considering β^{*2} and $\bar{h}_n(\sigma)$ influences on the distribution constant $D_{h,k}$ and on the weighting function distribution mean value: \bar{h}_w , which is also equal to the effective soil water potential for the linear soil water potential chosen for this study.

Figure E-15 shows $D_{h,k}$ plotted as a function of $\bar{\sigma}_h$ for four values of β^{*2} . Two aspects of the graphs are evident: (a) $D_{h,k}$ increases with increasing $\bar{\sigma}_h$

for each value of β^{*2} , and (b) $D_{h,k}$ tends toward unity, as β^{*2} decreases at all the values of $\bar{\sigma}_h$. It was previously indicated that $D_{h,k}$ is the integral of the product of the auxiliary potential function $\bar{u}_1(\sigma)$ and the radial transfer coefficient $\bar{h}_n(\sigma)$. The constant $D_{h,k}$ is therefore larger in situations where the σ - regions of larger values of $\bar{u}_1(\sigma)$, and larger values of $\bar{h}_n(\sigma)$ coincide, rather than where such regions are less overlapping. Figure E-16 illustrates the tendency in $\bar{u}_1(\sigma)$ to approach unity with decreasing β^{*2} and since $\bar{w}(\sigma)$ is proportional to the product of $\bar{u}_1(\sigma)$ and $\bar{h}_n(\sigma)$, the soil water potential weighting tends to be more and more dominated by the radial transfer coefficient distribution as $\beta^{*2} \rightarrow 0$. This fact is in agreement with the earlier observation for the special case of constant h and k_x .

The other important trend indicated in Figure E-16 is the tendency of $D_{h,k}$ to increase with increasing $\bar{\sigma}_h$. This tendency reflects the greater correspondence between the monotonically non-decreasing $\bar{u}_1(\sigma)$ and $\bar{h}_n(\sigma)$ for higher values of $\bar{\sigma}_h$. The effect on $D_{h,k}$ is much less at low values of β^{*2} since the total variation in $\bar{u}_1(\sigma)$ over $0 < \sigma \leq 1$ is also much lower, and keeping in mind that $D_{h,k} = 1$, in the limiting case $\beta^{*2} = 0$, regardless of the value of $\bar{\sigma}_h$.

Returning to the point of view that $\bar{u}_1(\sigma)$ is the axial water potential distribution associated with a hypothetical, reverse flow configuration, $D_{h,k}$ may be interpreted as an $\bar{h}_n(\sigma)$ weighted average of that hypothetical potential. In this sense $D_{h,k}$ is the weighted average axial potential value to which the radial flux would respond under a uniformly distributed, dimensionless soil water potential. The value of $D_{h,k}$ is both lower, and also more responsive to $\bar{\sigma}_h$, at high values of β^{*2} . This is a numeric indication of the expected degree of the "choking" effect of low k^* on the $\bar{\psi}_x$ and \bar{q}_x distributions already mentioned (Fig. E-3 and E-14).

Figures E-17 and E-18 show $\bar{\sigma}_w$ plotted as a function of $\bar{\sigma}_h$ for $\beta^{*2} = 0.1, 0.4, 1.6, \text{ and } 6.4$. At $\beta^{*2} = 0.1$ the relationship is nearly linear and differs only slightly from $\bar{\sigma}_w = \bar{\sigma}_h$. This characteristic of the graph coincides with the earlier observation that the weighting function $\bar{w}(\sigma)$ tends toward the radial transfer coefficient distribution as $\beta^{*2} \rightarrow 0$, regardless of the $\bar{h}_n(\sigma)$ function.

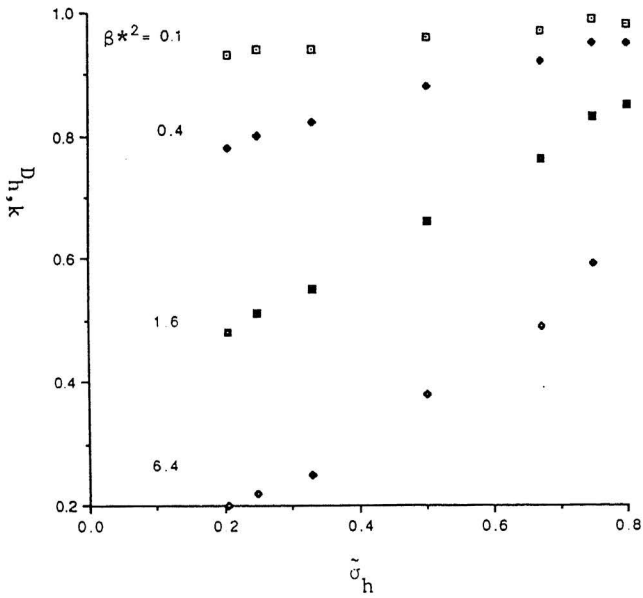


Fig.E-15 The Distribution Constant $D_{h,k}$ For Different Values of β^{*2}

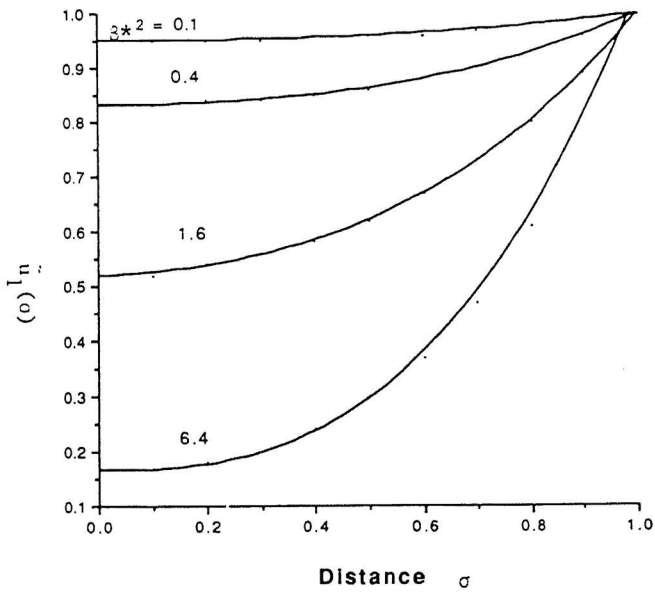


Fig.E-16 The Auxilliary Potential Function $\bar{u}(\sigma)$ for Different Values of β^{*2}

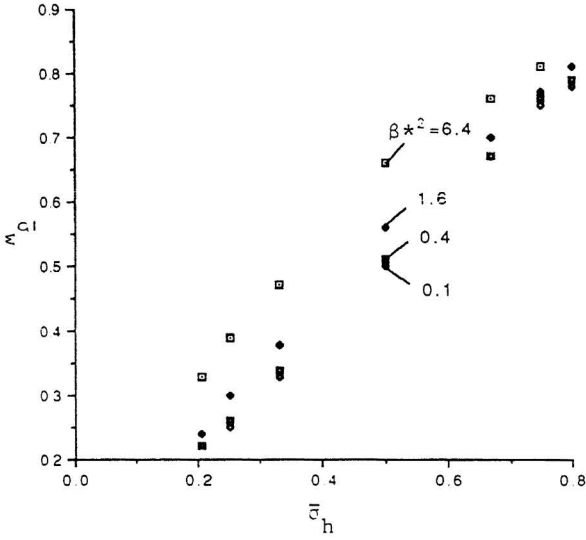


Fig.E-17 The Weighting Function Distribution Mean $\bar{\sigma}_w$ As a Function of $\bar{\sigma}_h$, For Different Values Of β^2

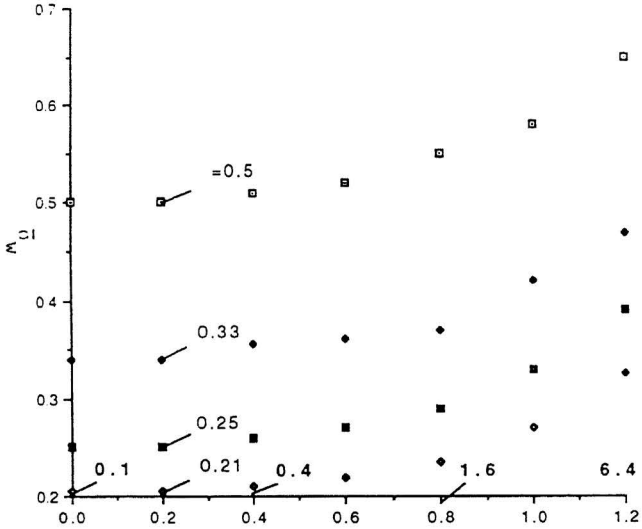


Fig.E-18 The Weighting Function Distribution Mean $\bar{\sigma}_w$, As A Function Of β^2 , For Different Values of $\bar{\sigma}_h$

Even at the higher values of β^{*2} , the relationship appears to be nearly linear, but there is a pronounced shift of $\bar{\sigma}_w$ to values higher than those of $\bar{\sigma}_h$ which reflects a shift of the zone of maximum weighting of $\tilde{w}(\sigma)$ toward the outflow boundary. Some deviation from linearity is observable for $\beta^{*2} > 1$, and the greatest deviation appears to be associated with the constant ($\bar{\sigma}_h = 0.5$) radial transfer coefficient distribution. This function is amodal, as opposed to the other more strongly monomodal functions in the set. (See Figures E-1 and E-2.)

From the point of view that the variable plotted on the vertical axis in Figure E-17 is $\tilde{\Psi}_s$ for the single soil water potential distribution, $\tilde{\psi}_s(\sigma) = \sigma$, two things are apparent. One is that the value of the effective soil water potential not only depends on $\tilde{\psi}_s(\sigma)$, per se, but also on the system hydraulic variables, β^{*2} and $\bar{\sigma}_h$. This is evident since $\tilde{\psi}_s(\sigma)$ was the same for all of the runs made. The above observation obviously carries over in general to any $\tilde{\psi}_s(\sigma)$ function. The second observation is merely that the effective soil water potential, as a number, carries information about the soil water potential distribution, but it also depends on properties of the root system and soil and the root zone which control h and k_x .

Remarks in this concluding paragraph apply to the reversal in direction of the axial flux that was discussed in the preceding section.

It occurred in association with a reversal in the lateral flux at the intersection of the $\tilde{\psi}_x$ graph with the $\tilde{\psi}_s$ graph. Figures E-19 and E-20 show the flux-reversal point σ^* and the maximum axial potential ψ_x^* plotted as functions of β^{*2} , for different values of $\bar{\sigma}_h$. As β^{*2} increases, the flux-reversal point shifts away from the outer extremity of flow region ($\sigma = 0$) toward the outflow boundary ($\sigma = 1$). Correspondingly, the maximum dimensionless potential increases from approximately 0.02 to values ranging from 0.15 to 0.30, as β^{*2} increases from 0.6 to 6.4.

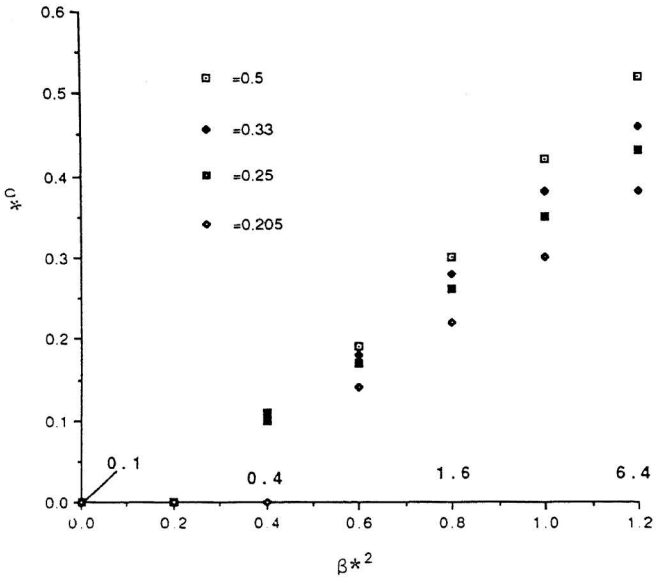


Fig.E-19 The zero flux point x_f^* , for different values of $\bar{\sigma}_h$

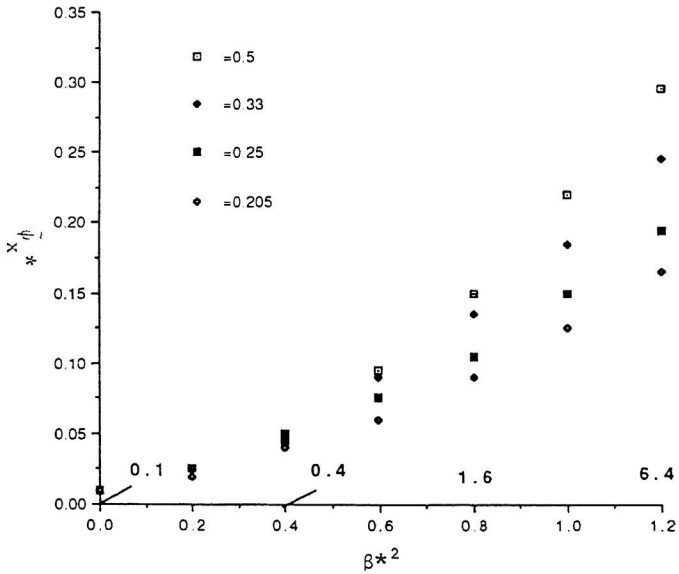


Fig.E-20 Maximum axial potential $x \psi_x^*$, for different values of $\bar{\sigma}_h$

Summary

The radial transfer coefficient distribution $\tilde{h}_n(\sigma)$ acts as a continuously variable "gate" over the full extent of the lateral boundary of the axial flow region: $0 < \sigma < 1$. The zone of maximum gating tends to be reflected by the first moment of the distribution function, $\bar{\sigma}_h$, for the set of functions considered in this analysis. For a given $\tilde{h}_n(\sigma)$, the axial potential, $\tilde{\psi}_x$, and axial flux, \tilde{q}_x , are noticeably affected by the total radial to axial conductance ratio, β^{*2} . For the assumed conditions of constant axial flux, a high value of β^{*2} reflects a uniformly distributed "choking" influence in the axial pathway (low k^*) in comparison to the relative rate of transfer across the boundary at a given potential difference. The choking effect leads to a steepening of the axial potential gradient near the outflow boundary, $\sigma = 1$, to a larger apportionment of the total potential difference, $\psi_s(y) - \psi_o$ toward the interior of the axial flow region. This latter difference may be written as $(\psi_s - \psi_x) + (\psi_x - \psi_o)$ and is shifted toward increasing dominance of $\psi_x - \psi_o$, with increasing β^{*2} .

Depending on the soil water potential distribution, an increase in β^{*2} may also lead to reverse flows (from the axial pathway into the surrounding soil) which increase in magnitude with increasing β^{*2} . The reverse flows are also strongly moderated by the value of $\bar{\sigma}_h$.

The system distribution constant, $D_{h,k}$, is a spatial distribution parameter of the product of the auxiliary potential function $\tilde{u}_1(\sigma)$ and the radial transfer coefficients distribution, $\tilde{h}_n(\sigma)$: $D_{h,k} = \int_0^1 \tilde{u}_1(\sigma) \tilde{h}_n(\sigma) d\sigma$. Since $\tilde{u}_1(\sigma)$ is a non-decreasing function, and since $\bar{\sigma}_h$ tracks the σ -region of high $\tilde{h}_n(\sigma)$, $D_{h,k}$ tends to be an increasing function of $\bar{\sigma}_h$. Its value reflects the degree of overlap of regions of high $\tilde{h}_n(\sigma)$ with those of high $\tilde{u}_1(\sigma)$. Values near unity occur in conjunction with low values of β^{*2} , since as $\beta^{*2} \rightarrow 0$, $\tilde{u}_1(\sigma) \rightarrow 1$ and $D_{h,k} \rightarrow 1$. $D_{h,k}$ decreases with increasing β^{*2} , but becomes more sensitive to $\bar{\sigma}_h$ as β^{*2} increases.

The first moment (mean σ -value) of the system weighting function is identical to the effective soil water potential when $\tilde{\psi}_s(\sigma) = \sigma$. Graphs of $\bar{\sigma}_w$ indicate that it is an approximately linear function of $\bar{\sigma}_h$ for low values of β^{*2} ; this is consistent with the observation that $\tilde{u}_1(\sigma) = 1$ and $\bar{w}(\sigma) \rightarrow \tilde{h}_n(\sigma)$ as $\beta^{*2} \rightarrow 0$. For the set of $\tilde{h}_n(\sigma)$ functions studied, the relationship was still approximately linear at high β^{*2} , but the graphs were shifted upward from $\bar{\sigma}_w = \bar{\sigma}_h$ with increasing β^{*2} and the greatest departure from linearity appeared to be associated with a constant function ($\bar{\sigma}_h = 0.5$).

Equal opportunity institution